# DESIGN, TESTING AND DEMONSTRATION OF A SMALL UNMANNED AIRCRAFT SYSTEM (SUAS) AND PAYLOAD FOR MEASURING WIND SPEED AND PARTICULATE MATTER IN THE ATMOSPHERIC BOUNDARY LAYER

**KEVIN DONALD ALEXANDER RIDDELL**
**BSc. Computer Science**
**University of Lethbridge, 2010**

A Thesis
Submitted to the School of Graduate Studies
of the University of Lethbridge
in Partial Fulfilment of the
Requirements for the Degree

**MASTER OF SCIENCE**

Department of Geography
University of Lethbridge
LETHBRIDGE, ALBERTA, CANADA

Approved:

| | (Print Name) | (Signature) | (Rank) | (Highest Degree) | Date |
|---|---|---|---|---|---|
| * | Supervisor | | | | |
| * | Thesis Examination Committee Member | | | | |
| * | Thesis Examination Committee Member | | | | |
| * | Thesis Examination Committee Member | | | | |
| * | External Examiner | | | | |
| * | Chair, Thesis Examination Committee | | | | |

## ABSTRACT

The atmospheric boundary layer (ABL) is the layer of air directly influenced by the Earth's surface and is the layer of the atmosphere most important to humans as this is the air we live in. Methods for measuring the properties of the ABL include three general approaches: satellite-based, ground-based and airborne. A major research challenge is that many contemporary methods provide a restricted spatial resolution or coverage of variations of ABL properties such as how wind speed varies across a landscape with complex topography. To enhance our capacity to measure the properties of the ABL, this thesis presents a new technique that involves a small unmanned aircraft system (sUAS) equipped with a customized payload for measuring wind speed and particulate matter. The research presented herein outlines two key phases in establishing the proof-of-concept of the payload and its integration on the sUAS: (1) design and testing and (2) field demonstration. The first project focuses on measuring wind speed, which has been measured with fixed wing sUASs in previous research, but not with a helicopter sUAS. The second project focuses on the measurement of particulate matter, which is a major air pollutant typically measured with ground-based sensors. Results from both proof-of-concept projects suggest that ABL research could benefit from the proposed techniques.

## ACKNOWLEDGEMENTS

This thesis could not have been completed without the help and support of many people. First, thank you Dr. Chris Hugenholtz and Dr. Derek Peddle for overseeing my research. A special thanks to my committee members Rob Laird and Mathew Letts for their help and scientific direction. Thank you to everyone at Windy West Flying Club for a safe location to conduct my research. A huge thanks to Heinz Fischer for all your assistance and support. Thanks to my peers, Devin Cairns, Tanya Byrne, James Banting, Logan Pryor, Peter Kennedy and Trevor Armstrong for the feedback and discussions which helped overcome research obstacles.

I would like to acknowledge all funders that (indirectly or directly) made this research possible: University of Lethbridge, Graduate Students Association, School of Graduate Studies, NSERC CREATE AMETHYST Program and Chris Hugenholtz.

A big thank you to my wonderful family including my amazing and beautiful wife Adria, my supportive and caring brother Kris, his wonderful wife Meghan, and Scott and Jan Ritchie for all their support and love. Thank you to my loving mother Ann and my always remembered and greatly missed father Don.

## TABLE OF CONTENTS

# LIST OF TABLES

# LIST OF FIGURES

## LIST OF ABBREVIATIONS

| | |
|---|---|
| ABL | Atmospheric Boundary Layer |
| AOD | Aerosol Optical Depth |
| CPU | Central Processing Unit |
| GCS | Ground Control Station |
| GND | Ground |
| GOES | Geostationary Operational Environmental Satellite |
| GRN | Green |
| GS | Ground Speed |
| IMU | Inertial Measuring Unit |
| KEI | Kinetic Energy on Impact |
| LiDAR | Light Detection and Ranging |
| MCS | Measurement and Control System |
| MODIS | Moderate Resolution Imaging Spectroradiometer |
| MTOW | Maximum Takeoff Weight |
| NMEA | National Marine Electronics Association |
| PM | Particulate Matter |
| $PM_{10}$ | PM smaller than 10 μm |
| PoC | Proof-of-Concept |
| PUF | Polyurethane Foam |
| RADAR | Radio Detection and Ranging |
| RC | Remote Controlled |
| Rx | Receiver |
| RXI | Receiver Input |
| SAHWSS | Small Autonomous Helicopter Wind Sensing System |
| SODAR | Sonic Detection and Ranging |
| sUAS | Small Unmanned Aircraft System |
| TAS | True Airspeed |
| TX | Transmit |
| TXO | Transmit Output |
| UAS | Unmanned Aircraft Systems |
| VTOL | Vertical Take-Off and Landing |

# CHAPTER 1: INTRODUCTION AND BACKGROUND

## 1.0 Motivation

The atmospheric boundary layer (ABL) is defined as the layer of air directly above the Earth's surface in which the effects of the surface (friction, heating and cooling) are felt directly on time scales less than a day, and in which significant fluxes of momentum, heat or matter are carried by turbulent motions on a scale of the order of the depth of the boundary layer or less (Garratt, 1994). The properties of the ABL, such as temperature, wind speed and humidity, have direct effects on a number of key processes that impact humans, including: wind energy, air quality and health, drifting snow, fog, among others. In the context of air quality, process such as dispersion, mixing, transformation, and deposition are dependent on the interaction between the Earth's surface and the ABL (Vilà-Guerau de Arellano et al., 2007). ABL winds change in accordance with varying Earth surface interactions. During these interactions particles are exchanged between the surface and the boundary layer and the Earth's surface becomes a source and storage for pollutants and various constituents. These aerosols can affect the quality of the air we breathe and the ability for the Sun's energy to pass to the Earth's surface (Team, 2005). These interactions between the biosphere and troposphere (air and aerosol movement) make this area of study important to understanding air quality issues and global climate change. A better understanding leading to better models could lead to tools to help predict future events.

Contemporary methods for measuring ABL properties include three general approaches: satellite-based, ground-based and airborne. Satellite-based methods include the use of passive and active sensors to measure properties like wind speed and particulate matter (PM). For example, wind speed can be calculated from ocean wave properties, as measured by the backscatter from microwaves transmitted by synthetic aperture radar sensors onboard satellites (e.g., ERS-2: Lehner et

al., 2000), whereas optical sensors like the Moderate Resolution Imaging Spectroradiometer (MODIS) can determine PM by measuring the degree to which the aerosols prevent the transmission of light in the atmosphere. Ground-based and in situ measurements include techniques such as tall masts with anemometers, or active remote sensing methods such as Doppler SODAR (Crescenti, 1997), radar (James, 1980) and LiDAR (Eberhard et al., 1980). Airborne measurements are acquired from flying platforms such as kites (Walesby et al., 2010), tethersonde, radiosonde balloons (Tapp et al., 1978), and piloted aircraft (Avissar et al., 2009).

Many of the above methods and techniques are commonly used to measure the ABL, but each has a certain limitation. For example, satellite methods tend to cover large areas but tend to have low spatial resolution, which makes it hard to pinpoint the small-scale variability that may be important for some applications. Airborne methods are either expensive (piloted aircraft) or can be cumbersome to operate (like kites and balloons). In situ methods also tend to lack portability (like tall towers), which makes it hard to measure spatial variations in ABL properties. One of the challenges, therefore, is to develop a method that is relatively inexpensive, easy to operate, and able to acquire accurate measurements at specified locations within the ABL.

In response to these issues, a new platform for ABL studies has begun to gain traction in atmospheric sciences. Small Unmanned Aircraft Systems (sUAS) are fully autonomous aircraft that are relatively inexpensive to purchase and operate compared to piloted aircraft, and able to carry small atmospheric measurement payloads. They can also operate at low altitudes near structures and landforms without the safety concerns that inhibit the use of manned aircraft in these situations. Over the past decade, a number of case studies have highlighted the potential of sUAS platforms for ABL measurements, most of which have focused on fixed-wing platforms (van den Kroonenberg et al., 2007; Lin et al., 2008; Mayer et al., 2010; Giebel et al., 2012; Bonin et al., 2013).

This thesis presents two proof-of-concept (PoC) investigations, each involving the design, testing and demonstration of an sUAS helicopter platform for measuring ABL properties. The first PoC investigation focuses on a custom wind speed measurement system, while in the second investigates a custom particulate matter (PM) measurement system. These ABL parameters were selected because they are important for air quality and involve sensors that have not been previously tested onboard sUASs. In the future, operational use of sUASs to measure wind speed and PM may be possible in key regions facing major air quality issues, like Alberta's oil sands (Kelly et al., 2009; Timoney et al., 2009). However, in order to establish the feasibility of this scenario, research is needed to establish the accuracy and viability of sUAS-based ABL measurements relative to conventional systems.

## 1.1 Background

In this section I will briefly examine the contemporary technology and methods used to measure ABL parameters. The technologies include both active and passive sensors for measuring ABL wind parameters and PM concentrations. sUAS platforms are discussed according to the history and recent uptake of sUAS platforms in scientific applications. The varying types, technologies and limitations are also examined.

## 1.2 Contemporary Sensors of ABL Measurements

### 1.2.1 In Situ Sensors

Many in situ technologies are used to measure ABL parameters. In regards to wind speed measurements, the most widely used technique is the cup anemometer, which is placed on a mast fixed to the ground. This simple yet robust sensor measures wind speed with high accuracy and low cost. Cup anemometers are subject, however, to over-speeding and slowdown errors in gusty

conditions and also lack the ability to discern wind direction. These over speeding and slowdown errors are caused by a nonlinear response in fluctuating winds (Busch et al., 1976). This is due to anemometers responding faster to a speed up in wind speed than an equivalent wind speed decrease, therefore wind speed will be overestimated. Given its long history in atmospheric studies the cup anemometer is the sensor of choice when testing and comparing to other ABL scientific instruments (Smith et al., 2006; Giebel et al., 2012).

The cup anemometer has been employed in a number of large-scale wind flow studies, often involving the deployment of an array of cup anemometers on tall masts. Notable examples include the Askervein Hill Project (Taylor et al., 1987) and the Bolund Experiment (Bechmann et al., 2009). However, due to the logistical requirements (i.e., anemometer array and number and heights of the masts), the experimental setup has not been duplicated frequently. Mast-mounted cup anemometers are also the formally-accepted sensor for wind speed when conducting a power performance test for wind turbine placement. Due to new hub heights exceeding 80 – 90 meters, mast structures must match this height for testing. These requirements have made using cup anemometers expensive and a logistically difficult choice (Courtney et al., 2008), often requiring the use of other sensors, like mini SODARs to measure wind speed above the mast.

Sonic anemometers measure wind speed by measuring travel time of ultrasound pulses in opposing directions (Schotland, 1955). High frequencies of 10-100 Hz allow turbulence measurements to be attained. Sonic anemometers have no moving parts, which make them an excellent choice for long term monitoring under harsh conditions (Giebel et al., 2012). However, sonic anemometers are typically not used on moving platforms like sUASs because the measurements are very sensitive to changes in the angle of the sensor. Unless an extremely accurate

inertial measurement unit is used to correct for changes in angle, mobile measurements with sonic anemometers are not very useful (Giebel et al., 2012).

### 1.2.2 Airborne Remote Sensing Platforms

A radiosonde is comprised of an untethered balloon and a measurement package. This platform is commonly used and has a long history of applications in atmospheric studies (DuBois et al., 2002). The payloads are specifically chosen for their application and can support a wide variety of sensors. Typical payloads consist of sensors for measuring atmospheric pressure, temperature, and moisture. The motion of the radiosonde is normally tracked and measured with a Global Positioning System (GPS). This tracking data can then be used in post processing to determine upper winds (Bailey, 2000).

Kites and tethered balloons offer an alternative airborne platform and are practical for a number of reasons. They can carry large payloads, several kilograms, capable of long-duration flights with pinpoint accuracy in the atmosphere, and are able to attain medium altitudes (~ 500 m) without fuel concerns. Kites do require a certain level of wind speed to generate lift (e.g., > 4 $ms^{-1}$; McGowan et al., 2008), they are able to measure vertical profiles and be controlled from the ground.

Piloted aircraft offer excellent platforms for atmospheric studies. These platforms allow for large payloads, high and low altitudes, and controlled flight paths to an area or event under study (Wandinger et al., 2002). Piloted aircraft are however very expensive to operate and maintain, and due to this reason, are not regularly used for research applications. They also pose substantial risk, especially in situations where the measurements of interest are in the lower region of the ABL.

### 1.2.3 Ground-Based Remote Sensing

Upward-pointing active sensors are commonly used to measure the ABL well-beyond the vertical extent of tall masts. Common ground-based remote sensing technologies include sonic

detection and ranging (SODAR), light detection and ranging (LiDAR), and radio detection and ranging (RADAR), all of which operate on the principle of measuring Doppler shift from either sound or electromagnetic waves.

SODAR operates on the principle of acoustic backscattering. Acoustic pulses are produced and directed into the atmosphere. As the sound wave moves through the atmosphere a small percentage of the energy is scattered by temperature heterogeneities whose scale is similar wavelength of the acoustic pulse. This scatter is collected by a receiver on the ground. This signal is sampled at a rate several hundred times per second over a period of several seconds. The Doppler shift or the difference in the frequencies between transmitted and backscatter is directly proportional to the radial wind velocity along the acoustic beam axis (Balser et al., 1976; Crescenti, 1997).

LiDAR is an active optical instrument, which sends a laser beam into the ABL, either in pulses or continuously. Reflection from aerosol particles in the atmosphere returns a portion of the signal back to the detector. Wind speed is derived from the Doppler shift of the returned signal. In addition to wind speed, LiDAR is also able to measure atmospheric elements such as clouds, aerosols, water vapour and temperature (Carswell, 1983; Weitkamp, 2005; Courtney et al., 2008).

RADAR also uses the Doppler shift method similar to the two methods presented above to measure the wind speed of PM entrained in the atmosphere. This is accomplished with the transmission, scattering and reflection of microwave radiation. Resultant backscattering from interaction with the atmosphere returns and a measured wind speed is derived (Browning et al., 1968).

Once the data are collected from one or several of the foregoing methods, the parameters are studied and used to develop models, which can be used to predict the state of atmospheric conditions in the future. Once a model is operational the only method for testing outputs are

through the contemporary ABL sensors currently in use; this is why new sensors and sensor combinations must be made to better test and verify the computational models. Through this ideology it is believed that as sensors become higher resolution and theories advance, the combination of new and different sensor types will result in synergistic benefits (Wilczak et al., 1996).

### 1.3 Small Unmanned Aircraft Systems

During the last decade a new sensor platform has emerged. The miniaturization of GPS receivers, magnetometers and inertial measurement units (IMUs) has directly affected the cost, size, and availability of UAS platforms. Examples of successful platforms in ABL studies include the Australian Aerosonde e.g., Holland et al. (2001), the $M^2AV$ e.g., Spiess et al. (2007), and the Small Unmanned Meteorological Observer (SUMO) e.g., Reuder et al. (2012).

Small Unmanned Aircraft Systems or sUASs are a class of autonomous aircraft, which are lighter than 25 kg (Hugenholtz et al., 2012). The class was developed to help formulate thresholds for the regulatory body issuing privileges to use an sUAS for commercial or scientific use. Anything at or below 25 kg maximum takeoff weight (MTOW) is considered safe and could attain insurance due to the amount of Kinetic Energy on Impact (KEI) if it were to strike a human (CCUVS, 2011). Technology to create sUASs originated in the military. Recent advances in GPS, IMUs and microprocessors make commercial- and scientific-grade systems possible and affordable.

Many different types of sUAS platforms exists. The main categories of sUASs are fixed-wing and rotary aircraft. Fixed-wing aircraft, or airplanes, usually have longer flight times, smaller payloads and must maintain a relatively fast forward velocity to maintain flight. They also typically require larger areas for take-off and landing. Rotary aircraft, or helicopters and quadcopters, normally have shorter flight times, higher payload capabilities, and don't need to maintain a forward velocity to

continue flight due to the innate hovering abilities. They also require very little space for take-off and landing (CCUVS, 2011). Commercial offerings of both are available but retrofitting hobby systems with autonomous capabilities is also possible by purchasing the parts separately.

To make autonomous flight possible, the required elements onboard an sUAS are:

- IMU: monitors the aircrafts roll, pitch and yaw.
- On board GPS: aircraft knows at what latitude and longitude it is positioned and its current ground speed.
- Magnetometer: position of the front of the aircraft.
- Central processing system: Processes flight parameters from onboard sensors and calculates new flying commands which are sent to the control surfaces. This process is a continuous feedback loop.
- Telemetry: Allows the ground control station (GCS) to communicate with the aircraft while it is in flight.

The most common sUAS platform currently used for ABL measurement studies are fixed-wing aircraft. Fixed-wing aircraft have been used to obtain vertical profiles of aerosols, temperature, dew point, and wind speed (van den Kroonenberg et al., 2007; Corrigan et al., 2008; Lin et al., 2008; Reuder et al., 2012; Bonin et al., 2013). Since a fixed-wing sUAS cannot hover and measure ABL properties at fixed points, researchers have relied on flying circular flight patterns. For upper wind measurements circular flight patterns ensure that the aircraft will experience a headwind and tailwind along two segments of the circle, thus allowing for calculation of wind speed and direction (van den Kroonenberg et al., 2008; Mayer et al., 2010). A major issue revealed by the sUAS literature is the accuracy of fixed-wing sUAS meteorological measurements, particularly regarding wind. Despite a vast number of publications, the error of sUAS wind measurements is not well quantified.

Helicopter platforms have been used in a limited number of meteorological studies and applications. It is not clear why so few studies have been conducted, however possible reasons could include the perception that they are more difficult to operate than fixed-wing aircraft, or that they have greater wake effects, which could contaminate measurements. Upon examining the literature for similar research it appears that helicopter platforms have been largely used in photogrammetry applications, some specialty aerosol sampling, and one ABL wind study, which failed to attain results (Eisenbeiss, 2004; McGonigle et al., 2008; Giebel et al., 2012).

The purpose of this research is to design and test a new helicopter-based sUAS platform for measuring wind speed and particulate matter, and if these components are successful, to then demonstrate the PoC. These ABL parameters were selected because they are directly relevant to air quality issues associated with open-pit mines in Alberta's Oil sands region (e.g., Kelly et al., 2009; Timoney et al., 2009). This thesis research represents an attempt to develop a technology that could assist in compliance auditing and air quality model testing. To the best of my knowledge, this research is novel in that no previous publication has reported the design, testing or demonstration of a similar platform and payload design.

## 1.4 Thesis Outline

This thesis is presented in a "manuscript style" and includes two core research chapters that each entails the technical and experimental design, key results, and a discussion of the main findings.

Chapter 2 outlines the design and test results of a new helicopter sUAS platform for measuring boundary-layer wind speed. First, the design of the custom measurement and control system (MCS) is presented and compared to a conventional logging system. Second, wake effects are examined to determine if the wind speed measured by the sUAS is commensurate to that measured

by a cup anemometer on a mast. Third, a series of wind profiles are presented as evidence for the PoC. The discussion highlights some of the advantages and limitations of the technology.

Chapter 3 builds on Chapter 2 and presents a similar workflow in terms of the design, testing and demonstration of payload for measuring PM in the ABL. In order to make the payload small, and therefore transferable to other sUASs, the first part of the research examines a lightweight commodity sensor (Sharp) for measuring PM, and its performance relative to a more expensive, heavier and widely used PM sensor (DustTrak). Results from a series of controlled tests demonstrate that the lightweight commodity sensor is not commensurate to the DustTrak. Therefore, in the second part of the research, the DustTrak is mounted to the sUAS and used to acquire vertical profiles of PM concentration, as well as in combination with the cup anemometer to measure PM flux.

## 1.5 References


Avissar, R., Holder, H. E., Abehserra, N., Bolch, M. A., Canning, P., Magalhaes, J., . . . Prince, K. (2009). The Duke University helicopter observation platform. *Bulletin of the American Meteorological Society, 90*(7), 939-954.

Bailey, D. T. (2000). *Meteorological monitoring guidance for regulatory modeling applications*: DIANE Publishing.

Balser, M., McNary, C. A., Nagy, A. E., Loveland, R., & Dickson, D. (1976). Remote wind sensing by acoustic radar. *Journal of Applied Meteorology, 15*(1), 50-58.

Bechmann, A., Berg, J., Courtney, M., Ejsing Jørgensen, H., Mann, J., & Sørensen, N. N. (2009). *The Bolund experiment: overview and background*: Danmarks Tekniske Universitet, Risø Nationallaboratoriet for Bæredygtig Energi.

Bonin, T., Chilson, P., Zielke, B., & Fedorovich, E. (2013). Observations of the Early Evening Boundary-Layer Transition Using a Small Unmanned Aerial System. (0006-8314). Retrieved 2013/01/01, from Springer Netherlands http://dx.doi.org/10.1007/s10546-012-9760-3

Browning, K. A., & Wexler, R. (1968). The determination of kinematic properties of a wind field using Doppler radar. *Journal of Applied Meteorology, 7*(1), 105-113.

Busch, N. E., & Kristensen, L. (1976). Cup anemometer overspeeding.

Carswell, A. I. (1983). Lidar measurements of the atmosphere. *Canadian Journal of Physics, 61*(2), 378-395.

CCUVS. (2011). *Unmanned: Textbook for UAS Studies* (1st Edition ed.). Ottawa, Ontario: Aviation Publishers Co. Ltd.

Corrigan, C. E., Roberts, G. C., Ramana, M. V., Kim, D., & Ramanathan, V. (2008). Capturing vertical profiles of aerosols and black carbon over the Indian Ocean using autonomous unmanned aerial vehicles. *Atmospheric Chemistry and Physics, 8*(3), 737-747.

Courtney, M., Wagner, R., & Lindelöw, P. (2008). *Testing and comparison of lidars for profile and turbulence measurements in wind energy*. Paper presented at the IOP Conference Series: Earth and Environmental Science.

Crescenti, G. H. (1997). A Look Back on Two Decades of Doppler Sodar Comparison Studies. *Bulletin of the American Meteorological Society, 78*(4), 651-673.

DuBois, J. L., Multhauf, R. P., & Ziegler, C. A. (2002). The Invention and Development of the Radiosonde with a Catalog of Upper-Atmospheric Telemetering Probes in the National Museum of American History, Smithsonian Institution. *Smithsonian*.

Eberhard, W. L., & Schotland, R. M. (1980). Dual-frequency Doppler-lidar method of wind measurement. *Applied Optics, 19*(19), 2967-2976.

Eisenbeiss, H. (2004). A mini unmanned aerial vehicle (UAV): system overview and image acquisition. *International Archives of Photogrammetry. Remote Sensing and Spatial Information Sciences, 36*(5/W1).

Garratt, J. R. (1994). *The atmospheric boundary layer*: Cambridge university press.

Giebel, G., U., Schmidt P., Bange, J., La Cour-Harbo, A., Reuder, J., Mayer, S., . . . Mølgaard, J. (2012). Autonomous Aerial Sensors for Wind Power Meteorology-A Pre-Project: Danmarks Tekniske Universitet, Risø Nationallaboratoriet for Bæredygtig Energi.

Holland, G. J., Webster, P. J., Curry, J. A., Tyrell, G., Gauntlett, D., Brett, G., . . . Vaglienti, W. (2001). The Aerosonde Robotic Aircraft: A New Paradigm for Environmental Observations. *Bulletin of the American Meteorological Society, 82*(5), 889-901.

Hugenholtz, C. H., Moorman, B. J., Riddell, K., & Whitehead, K. (2012). Small unmanned aircraft systems for remote sensing and earth science research. *Eos, Transactions American Geophysical Union, 93*(25), 236-236.

James, P. K. (1980). A review of radar observations of the troposphere in clear air conditions. *Radio Science, 15*(2), 151-175.

Kelly, E. N., Short, J. W., Schindler, D. W., Hodson, P. V., Ma, M., Kwan, A. K., & Fortin, B. L. (2009). Oil sands development contributes polycyclic aromatic compounds to the Athabasca River and its tributaries. *Proceedings of the National Academy of Sciences, 106*(52), 22346-22351.

Lehner, S., Schulz-Stellenfleth, J., Schattler, B., Breit, H., & Horstmann, J. (2000). Wind and wave measurements using complex ERS-2 SAR wave mode data. *Geoscience and Remote Sensing, IEEE Transactions on, 38*(5), 2246-2257.

Lin, P. H., & Lee, C. S. (2008). The eyewall-penetration reconnaissance observation of Typhoon Longwang (2005) with unmanned aerial vehicle, Aerosonde. *Journal of Atmospheric and Oceanic Technology, 25*(1), 15-25.

Mayer, S., Sandvik, A., Jonassen, M. O., & Reuder, J. (2010). Atmospheric profiling with the UAS SUMO: a new perspective for the evaluation of fine-scale atmospheric models. *Meteorology and Atmospheric Physics, 116*(1-2), 15-26.

McGonigle, A. J. S., Aiuppa, A., Giudice, G., Tamburello, G., Hodson, A. J., & Gurrieri, S. (2008). Unmanned aerial vehicle measurements of volcanic carbon dioxide fluxes. *Geophysical Research Letters, 35*(6), L06303.

Reuder, J., Jonassen, M. O., & Ólafsson, H. (2012). The Small Unmanned Meteorological Observer SUMO: Recent developments and applications of a micro-UAS for atmospheric boundary layer research. *Acta Geophysica, 60*(5), 1454-1473.

Schotland, R. M. (1955). The measurement of wind velocity by sonic means. *Journal of Meteorology, 12*(4), 386-390.

Smith, D. A., Harris, M., Coffey, A. S., Mikkelsen, T., Jørgensen, H. E., Mann, J., & Danielian, R. (2006). Wind lidar evaluation at the Danish wind test site in Høvsøre. *Wind Energy, 9*(1-2), 87-93.

Spiess, T., Bange, J., Buschmann, M., & Vörsmann, P. (2007). First application of the meteorological Mini-UAV 'M2AV'. *Meteorologische Zeitschrift, 16*(2), 159-169.

Tapp, R. G., & Lile, R. C. (1978). A new tethersonde system for remote measurement of wind and temperature. *Boundary-Layer Meteorology, 15*(4), 465-479.

Taylor, P. A., & Teunissen, H. W. (1987). The Askervein Hill project: overview and background data. *Boundary-Layer Meteorology, 39*(1-2), 15-39.

Team, ESRL Web. (2005). ESRL Themes: Surface and Planetary Boundary Layer Processes. from http://www.esrl.noaa.gov/research/themes/pbl/

Timoney, K. P., & Lee, P. (2009). Does the Alberta tar sands industry pollute? The scientific evidence. *Open Conservation Biology Journal, 3*, 65-81.

van den Kroonenberg, A., Martin, T., Buschmann, M., Bange, J., & Vörsmann, P. (2008). Measuring the Wind Vector Using the Autonomous Mini Aerial Vehicle M2AV. *Journal of Atmospheric and Oceanic Technology, 25*(11), 1969-1982.

van den Kroonenberg, A., Spieß, T., Buschmann, M., Martin, T., Anderson, P. S., Beyrich, F., & Bange, J. (2007). Boundary layer measurements with the autonomous mini-UAV M 2 AV. *Proceedings of DACH2007, Hamburg, Germany*, 10-14.

Vilà-Guerau de Arellano, J., Jonker, H., Pino, D., Ten Brink, H. M., Chaumerliac, N., Faloona, I., . . . Stutz, J. (2007). The Role of Atmospheric Boundary Layer Processes in Atmospheric Chemistry. *Bulletin of the American Meteorological Society, 88*(8), 1245-1248.

Walesby, K. T., & Harrison, R. G. (2010). Note: A thermally stable tension meter for atmospheric soundings using kites. *Review of Scientific Instruments, 81*(7), 076104-076104-076103.

Wandinger, U., Müller, D., Böckmann, C., Althausen, D., Matthias, V., Bösenberg, J., . . . Stohl, A. (2002). Optical and microphysical characterization of biomass-burning and industrial-pollution aerosols from-multiwavelength lidar and aircraft measurements. *Journal of Geophysical Research: Atmospheres (1984–2012), 107*(D21), LAC 7-1-LAC 7-20.

Weitkamp, C. (2005). *Lidar: range-resolved optical remote sensing of the atmosphere* (Vol. 102): Springer.

Wilczak, J. M., Gossard, E. E., Neff, W. D., & Eberhard, W. L. (1996). Ground-based remote sensing of the atmospheric boundary layer: 25 years of progress. *Boundary-Layer Meteorology, 78*(3-4), 321-349.

# CHAPTER 2: ATMOSPHERIC WIND EVENT MEASURING WITH A SMALL UNMANNED AIRCRAFT SYSTEM (SUAS)

## 2 Abstract

Small unmanned aircraft systems (sUASs) could be a viable option for measuring atmospheric properties in the absence of other ground-based or aerial techniques. To date, most research on this topic has focused on fixed-wing sUASs, but for some boundary-layer properties like wind, there are applications that may benefit from using a platform that can maintain a fixed position. Here, the design and test results of a new helicopter sUAS platform for measuring boundary-layer wind speed are presented. The motivation for this research was to develop a system that could be deployed in an operational capacity to measure event-based wind speed in hard-to-reach locations, like near structures or in complex terrain. The objective of this paper is to demonstrate the proof-of-concept (PoC) and to show the accuracy and limitations of the system. The system consists of an Align T-Rex 700 helicopter equipped with a DJI Ace Waypoint autopilot and a customized wind measurement payload. The latter makes up the measurement and control system (MCS). It uses an Arduino microcontroller with GPS and a cup anemometer attached to the end of a long boom extending in front of the aircraft. The performance of the custom wind measurement payload was tested against a conventional logging system comprising a Campbell Scientific CR1000 datalogger and RM Young cup anemometer. Results show a near 1:1 relation between the two systems. Wake effects during flight were also tested by comparing in-flight wind speeds from the sUAS to those measured by an anemometer fixed to an adjacent tower; again, the result was approximately 1:1, implying no wake effects. The operational use of the system for measuring wind speed profiles was also demonstrated, and shows that even under strong winds (18 m/s) the platform is stable and capable of maintaining its position within 1 m of a prescribed waypoint. Finally, a discussion of the

performance of this new sUAS wind measurement system relative to other small autonomous systems is presented, as well as some of the advantages and disadvantages of this system for operational boundary-layer wind measurement.

## 2.0 Introduction

Continuous and event-based measurements of the atmospheric boundary layer (ABL) wind have progressed in the last 50 years through innovations in ground-based, airborne, and satellite methods. However, some major limitations persist in terms of measuring the spatio-temporal variability of ABL properties in an operational capacity. For example, tower-based systems continue to dominate the global array of meteorological networks, but they typically lack the ability to capture the vertical variations of wind above 10 m, and are incapable of synthesizing horizontal variations that result from topography and surface features. In situ profilers based on SODAR, LiDAR or RADAR technology can extend the reach of towers, and in many pragmatic applications the two approaches are used in tandem, but like towers profilers generally lack the ability to characterize horizontal variability. Similarly, tethered balloons, kites and various forms of sondes are useful for profiling, but most are cumbersome and not regularly deployed for operational purposes. Despite these challenges, ABL measurements remain a top priority for a variety of pragmatic applications, including: pollution measurement, wind energy assessment, built environment aerodynamics, and severe storm monitoring. Thus, measurement technology that is capable of measuring vertical and horizontal variations of wind speed remains a top priority.

One alternative to the suite of methods listed above is to use piloted aircraft. This type of platform has been used in numerous meteorological applications, but most measurement campaigns are undertaken with large fixed-wing platforms well above the ABL. For smaller footprints, piloted helicopters afford an excellent platform from which to measure various ABL parameters (Avissar et

al., 2009) but in general, most forms of piloted aircraft are expensive to operate and as such, they are not routinely used in ABL research or professional practice. In response to the foregoing challenges, researchers have been experimenting with small unmanned aircraft systems (sUASs). These platforms are considerably less expensive to purchase and operate compared to piloted aircraft, which makes them highly accessible for research and applied applications. They also offer greater flexibility and reduced risk for measuring ABL wind flow. Over the past decade, a number of case studies have highlighted the potential of UASs for event-scale ABL measurements, most of which are based on fixed-wing platforms (Reuder et al., 2008; van den Kroonenberg et al., 2008; Thomas et al., 2011).

For most ABL parameters the main challenge is simply to position a sensor at a desired height and acquire the wind speed measurement. In this regard, the type of platform doesn't matter, so long as it attains the desired position and records the data. However, research has shown that wind speed measurement with sUASs is not as straightforward as it might seem. Fixed-wing sUASs used for measuring wind typically incorporate a pitot-static system to derive the aircraft's true airspeed (TAS), which is the speed of the aircraft relative to the air around it. It calculates this by measuring the pressure differential between ram air from the pitot-tube, and static air from the static port. The greater the pressure differential, the greater the speed of the sUAS system; therefore, the airspeed is derived from the difference in dynamic and static air pressure (van den Kroonenberg et al., 2008). UASs built on this principle measure the change between the pitot-derived TAS and the ground speed (GS) with the latter is determined by the aircraft's GPS (Reuder et al., 2008). Using this approach a wind vector is derived only if the aircraft flies in a circular or helical pattern as all directions must be sampled prior to deriving a wind vector.

Flying helical patterns in order to derive the wind vector provides one measurement for a full 360° turn, which limits the ability to record changing characteristics of ABL wind at high spatial and temporal resolution. Depending on the speed of the aircraft and the time it takes to perform a 360° turn, it could take several minutes to derive one data point. An example of this comes from an ABL study conducted in Antarctica with a fixed-wing sUAS (van den Kroonenberg et al., 2008), whereby 7 wind speeds were measured at 4 altitudes during a 30 minute flight.

The authors reported that the sources of uncertainty affecting wind speed values derived with this method could include up to eight different factors. Major contributors of error are generated by unwanted aircraft velocity or movement in different planes of motion, such as roll, pitch, and yaw, which occur due to turbulence and the aircraft's response to turbulence as it flies its predefined route. Other sources of error come from pitot tube installation and instrument error (Koçer, 2012). These errors can dramatically affect the platform's ability to collect accurate data. Similarly, NOAA's Tempest UAS was designed to observe and target severe local storms, providing event-based wind estimates, but the quality of the estimates were far from meeting the requirements needed to be considered science-grade (Frew et al., 2012). Fixed-wing sUASs also require space or specialty equipment to take off and land and aren't able to measure ABL parameters low to the ground, close to trees, or in confined places.

A helicopter sUAS may provide an excellent alternative to fixed-wing sUASs for collecting ABL parameters. Helicopters are able to operate in limited spaces, and as such, are able to fly to desirable collection locations, establish hover and acquire measurements. These flying characteristics make helicopters ideal around structures, complex terrain, and in forested regions. Measurements close to the ground and around complex structures are important as the spatial variability of the Earth's surface has considerable impact on the atmosphere at all scales and observing the physical

and chemical properties of the atmosphere near the Earth's surface remains a great challenge (Avissar et al., 2009). Understanding these processes and interactions will allow us to better model and parameterize these practices and understand our changing environment.

The purpose of this research is to examine a new sUAS platform and data collection system specifically-designed for measuring ABL wind speed. The platform consists of a traditional helicopter built using a T-Rex 700N hobby kit (ALIGN, Taiwan) which was paired with a DJI Ace Waypoint autopilot (DJI, Hong Kong, China). The data collection system was created using an Arduino microprocessor, which is an open source prototyping platform, and a NovaLynx digital cup anemometer. The collection system was built and tested to accepted methods in the literature (e.g., Sotelino et al., 2012) and was compared in two experiments: first in situ, then in flight. The platform was designed to allow pinpoint wind measurements in complex terrain and environments. Wind speed was selected as it has proved to be one of the most difficult parameters to measure accurately and current methods using sUASs rely on fixed-wing platforms.

### 2.1 Background: UAS

UAS systems were initially developed for use in military operations. In the early 1990s and 2000s civilian scientific experimentation with UAS systems began in earnest. Recently, the costs and availability of components to make hobby-grade radio-controlled (RC) aircraft autonomous has decreased substantially, which has made UAS technology accessible to the masses (Holland et al., 1992; Daida et al., 1994; Egger et al., 2000; Holland et al., 2001). RC aircraft are controlled from the ground using a transmitter with a frequency-matching the receiver in the aircraft. The receiver is used to communicate with the flight controls, which are manually controlled by a pilot on the ground. Autopilot systems in UASs replace the manual procedures involved in flying RC aircraft, thus enabling greater focus on data acquisition rather than how the aircraft is operated. Autopilot

systems consist of a central processing unit (CPU), which integrates with the flight controls to allow hardware in the loop flight decisions. The CPU makes decisions on information derived from an Inertial Measuring Unit (IMU), which relays the current orientation of the aircraft. A magnetometer, which sends the current heading, paired with a GPS, informs the CPU of the aircraft's current position, ground speed and direction. Most UAS systems also have telemetry, which allows communication with the aircraft as it flies. This connection permits two-way communications with the UAS, giving the user the ability to upload new directives during the flight. Telemetry also provides the ability to maintain watch of the aircraft's status and mission progression.

The majority of sUASs used in ABL studies have been fixed-winged aircraft. This is likely due to their simplicity of design, ease of use and low cost. Current ABL parameters studied using an sUAS include wind, temperature, pressure and humidity (van den Kroonenberg et al., 2007; Corrigan et al., 2008; Lin et al., 2008; Reuder et al., 2012; Bonin et al., 2013). While some platforms are being used operationally for different meteorological applications, the majority of research is still in a proof of concept phase (van den Kroonenberg et al., 2008; Reuder et al., 2009). One important issue revealed by the literature is the accuracy of meteorological measurements, particularly wind, with sUAS platforms. Despite many publications, the error of sUAS wind measurements is not well quantified. Refocusing on this issue will help refine the science and hopefully lead into more applied research.

## 2.2 Methodology:

### 2.2.1 sUAS Platform Specifications

In order to overcome some of the challenges identified with fixed-wing sUASs, we designed a helicopter-based measurement unit based on a T-Rex 700N, which is a hobbyist nitro-powered traditional helicopter system. The 700N is a flybarless (a two-bladed rotor system that does not have

a flybar to help stabilize) 7-channel helicopter system with a 1562 mm main rotor diameter and a tail rotor diameter of 281 mm (Figure 2.1). The rigid frame design is built with carbon fiber. The helicopter is power by a .91 cu. in. nitro engine producing roughly 4 HP. The empty weight of the aircraft is 9.04 lbs. and the total length is 1335 mm. The platform was selected because of the distinctive flying characteristics produced by a helicopter system. These skills include low flying capabilities, ability to hover, and vertical takeoff and landing. The helicopter platform is also able to carry a significant payload in almost any shape or size as maintaining aerodynamic flow is not of concern for flight. It is not clear why helicopter sUASs have not been used extensively prior to this research. Reasons could include the level of operating difficultly compared to fixed-wing aircraft, or the misconception that they have greater wake effects, which could contaminate measurements. Research on helicopter aerodynamics has shown, however, that in hover the downwash wake angle is vertical, which means that placement of the sensor to measure wind speed must project beyond the rotor tip (Figure 2.1) (Glauert, 1935; Conlisk, 1997; Avissar et al., 2009). This distance beyond the rotor will decrease with increased velocity in forward flight or in higher wind conditions as airflow pushes the area of influence from the rotor wash downwind.

Figure 2.1. Profile view of the sUAS. The boom with anemometer is mounted forward of the flying surfaces to minimize wake turbulence. The collection payload is located just forward of main mast as close as possible to center of gravity to maintain positive flying characteristics.

### 2.2.2 Payload: Wind Sensor

The wind sensor needed to be small and light in order to operate on the sUAS platform. One of the main requirements of the system is to accurately measure wind speed while on a dynamic platform. Since the platform moves, limitations exist on what types of wind sensors were able to be used. Sonic anemometers require a stable platform or the ability to resolve movement and orientation at high frequency. To determine these movements a very precise IMU is required. For this research, the IMU would need to be small, accurate, and affordable to rectify the data. An IMU satisfying these requirements has yet to be found. Risø National Laboratory for Sustainable Energy, a Technical University in Denmark, attempted a similar method. They used a helicopter platform with a sling load collection package comprising a sonic anemometer and Xsens MTiG Inertial

Navigation System. Results from their research are unclear, however, as they were not able to attain more than 80 seconds of data (Giebel et al., 2012). The pitot static system, which is commonly used on fixed-wing UASs, was not considered as these sensors must always be pointed directly into the wind. Another technique to measure wind speed involves hot-wire anemometry. These sensors use a very fine wire that is electrically heated to a temperature above ambient. As air passes the wire the cooling effect is measured through the metals dependency on temperature and resistance. Knowing this relationship, the wind speed can be determined. Hot-wire anemometers are extremely thin and delicate and can easily be damaged by insects and larger particles making them impractical on a UAS (Giebel et al., 2012).

Due to its simplicity and effectiveness, the wind sensor selected for our platform was a cup anemometer (Figure 2.1). This sensor was chosen as it has a long and established history for measuring wind speed, thus we maintain commensurability with conventional tower-based measurements. Though it lacks the ability to parameterize 3D turbulence like a sonic anemometer, the rotational cup anemometer's simplicity, durability, and precision make it excellent for application on a dynamic platform. At this point in the research the only unknown factor regarding the cup - anemometer is whether it records false values induced by the wake from the helicopter during flight. We thus tested its performance against another anemometer fixed to a tower.

The cup anemometer used for measuring wind speed was the NovaLynx 200-WS-01 wind speed sensor. The NovaLynx accuracy is 0.2 m/s with a speed threshold of 0.35 m/s and is capable of measurements up to 44.3 m/s. It uses a reed switch, which produces a digital signal every time the reed switch passes a magnet and closes the connection. This occurs three times for every rotation of the anemometer. An undesirable situation can occur with reed switches as some reed switches may bounce when passing the magnet. This will induce several false signals in one rotation. Methods for

dealing with such a situation can either be through software or hardware solutions. The hardware method involves building another circuit using a capacitor, two resistors, and a diode. This circuit works such that when the reed switch is activated, the capacitor charges with current from the system. The digital input pin reads "High" at this time and the capacitor stays charged until the switch is opened. At this time the capacitor discharges through the two resistors. Once it's discharged, the voltage is near 0 and the digital input pin reads "Low". Software methods to eliminate a bouncy reed switch involve using timers to eliminate multiple signals being counted as data. Though software methods can work, they are not always assured to work due to changing speeds in which the reed switch is triggered.

### 2.2.3 Payload: Measurement and Control System (MCS)

The datalogger used in this investigation was designed to be compact, lightweight, robust, and capable of measuring the NovaLynx digital signal, as well as the data from a GPS. Few dataloggers used for meteorological measurements meet these criteria. As such, we developed a custom MCS with the Arduino Mega 2650 prototyping platform (Figure 2.2). Arduino is an open-source electronics platform based on flexible, easy-to-use hardware and software. Arduino boards are designed to combine with many different sensors and integrate in specific ways through code in the Arduino Integrated Development Environment. The microcontroller on the Arduino board is programmed using the Arduino programming language, which is based on the Wiring language. Processor, memory, and input requirements for the datalogger were also taken into consideration when choosing an Arduino board and future expandability for other sensors. Expansion boards were used to remove the use of prototyping breadboards and to keep the system compact and free of loose wires (Figure 2.2). One of the expansion boards connected the onboard GPS and microSD data card for storing wind speed and GPS data. The second expansion board connected the power, a small LCD screen that displays data in real-time, and the anemometer. The Wiring program that was

used for this experiment can be seen in Appendix 1, Arduino Program.

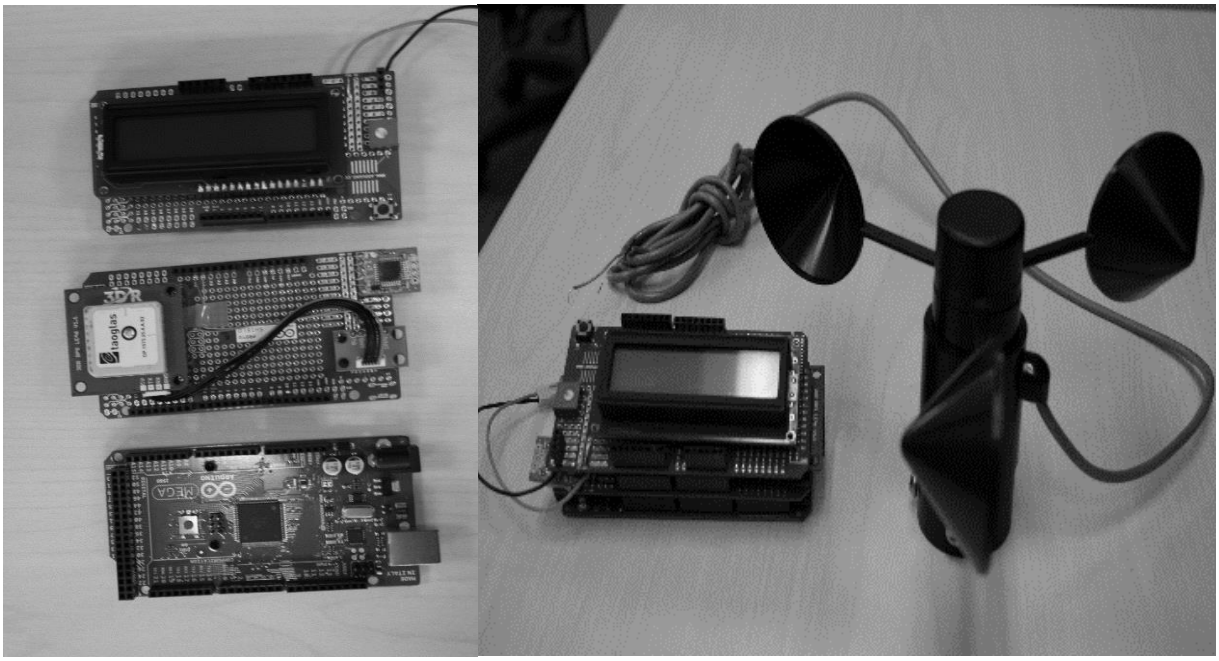

Figure 2.2 The Arduino-based MCS and expansion boards. Left: the complete MCS. Right: the MCS and NovaLynx 200-WS-01 digital anemometer.

As a GPS receiver we used Ublox LEA-6H. Connecting this module to the Arduino Mega was accomplished through a breakout board that supports a MTK cable and adapter. The breakout board allowed the GPS to be tethered to the Arduino by a cable, which provided better positioning of the GPS, thus reducing signal attenuation. The GPS breakout board connected to the Arduino system via four solder connections, receiver (Rx), transmit (TX), ground (GND), and power (5V).

Communication with the GPS receiver was achieved using a software library. The library, TinyGPS, requires the GPS receiver to output the NMEA sentence structure. TinyGPS allows the user to easily select which elements are received and stored from the NMEA sentence. GPS code continually runs and updates as the anemometer spins and collects new wind data every 1 Hz. As

wind data are collected, new position values are stored alongside. All but the wind data values are derived from the GPS receiver. The NMEA sentence provides latitude, longitude, altitude, time and number of satellites connected.

The NMEA string includes many important parameters suitable for a variety of uses, however, for this project the focus is the time and 3D coordinates. Other parameters, such as number of connected satellites are included to add confidence in the data acquired. NMEA sentence structure contains 19 different sentence identifiers followed by a string that contains included information (Table 2.1). The relevant strings used in creating this mobile wind datalogger are $GPGGA, $GPGSV, and $GPZDA, with the majority of the data coming from the $GPGGA string.

Table 2-1. Details of the $GPGGA header sentence. As $GPGGA information is sent from the GPS to the Arduino at 1 Hz, it is checked to see if information has changed, if information is new it is parsed and used for new wind parameters being saved.

| **Name** | **Example Data** | **Description** |
|---|---|---|
| Sentence Identifier | $GPGGA | Global Positioning System Fix Data |
| Time | 170834 | 17:08:34 Z |
| Latitude | 4124.8963, N | 41d 24.8963' N or 41d 24' 54" N |
| Longitude | 08151.6838, W | 81d 51.6838' W or 81d 51' 41" W |
| Fix Quality:<br>0 = Invalid<br>1 = GPS fix<br>2 = DGPS fix | 1 | Data is from a GPS fix |
| Number of Satellites | 05 | 5 Satellites are in view |
| Horizontal Dilution of Precision (HDOP) | 1.5 | Relative accuracy of horizontal position |
| Altitude | 280.2, M | 280.2 meters above mean sea level |
| Height of geoid above WGS84 ellipsoid | -34.0, M | -34.0 meters |
| Time since last DGPS update | Blank | No last update |
| DGPS reference station id | Blank | No station id |
| Checksum | *75 | Used by program to check for transmission errors |

The OpenLog breakout board was used with the Arduino platform to record wind speed and related GPS data. OpenLog has six solder points, of which only five are necessary to connect the device to the Arduino. The connection points required are green (GRN) which is connected to the reset switch on the Arduino, which when clicked, tells the OpenLog to begin recording the input stream into a new file. Receiver input (RXI) connected to one of the Arduino Mega serial transmit (TX) ports. Transmit output (TXO) was connected to an Arduino Mega serial input port, while voltage common cathode (VCC) was connected to 3.3-volt power connection, and ground (GND) was connected to ground on the Arduino board. Code was not required to make the logger work and record data; rather any data that are sent to the serial port, " *Serial.println (output);* " through the serial print command, are saved on the SD card. An example of the output is shown in Table 2.2.

Table 2-2. Example of the raw data recorded by the MCS and saved to SD card.

| Wind Speed (m/s) | Time (UTC) | Latitude | Longitude | Altitude (ASL) | Satellites | Number |
|---|---|---|---|---|---|---|
| 1.5 | 17:22:55 | 49.68087 | -112.870399 | 939.1 | SAT=11 | 4204 |
| 2.25 | 17:22:56 | 49.68087 | -112.870399 | 939.4 | SAT=11 | 4205 |
| 1.5 | 17:22:57 | 49.68087 | -112.870399 | 939.4 | SAT=11 | 4206 |
| 1.5 | 17:22:58 | 49.68087 | -112.870399 | 940 | SAT=10 | 4207 |
| 2.25 | 17:22:59 | 49.68087 | -112.870399 | 940.3 | SAT=10 | 4208 |
| 3 | 17:23:00 | 49.68087 | -112.870399 | 940.6 | SAT=10 | 4209 |
| 1.5 | 17:23:01 | 49.68087 | -112.870399 | 940.8 | SAT=11 | 4210 |
| 2.25 | 17:23:02 | 49.68087 | -112.870399 | 940.8 | SAT=10 | 4211 |
| 1.5 | 17:23:03 | 49.68087 | -112.870399 | 940.8 | SAT=10 | 4212 |
| 3 | 17:23:04 | 49.68087 | -112.870407 | 941.1 | SAT=11 | 4213 |
| 3 | 17:23:05 | 49.68087 | -112.870407 | 941.2 | SAT=11 | 4214 |
| 3 | 17:23:06 | 49.680858 | -112.870407 | 941.4 | SAT=11 | 4215 |
| 3 | 17:23:07 | 49.680858 | -112.870407 | 941.9 | SAT=11 | 4216 |
| 3 | 17:23:08 | 49.680858 | -112.870407 | 942.1 | SAT=11 | 4217 |
| 1.5 | 17:23:09 | 49.680858 | -112.870407 | 942.1 | SAT=11 | 4218 |
| 2.25 | 17:23:10 | 49.680858 | -112.870407 | 941.9 | SAT=11 | 4219 |

The Arduino Mega 2560 microcontroller is compatible with a range of battery sources: 7 to 12 Volts are recommended, but it is capable of operating from 6 to 20 Volts. The original battery type

selected was an 11.1 Volt lithium polymer battery (LiPo). LiPo power source was selected because of its size, weight, ability to produce significant power, and its ability to recharge in a short period of time. The battery was able to power the system for 15 hours, but upon complete discharge the battery was not able to charge again and needed to be replaced. Due to this issue, a lithium iron polymer battery was used that could be completely drained and would allow another charge. Systems onboard the Arduino operate at either 5-volts or 3.3-volts. Preference is given to 3.3-volt systems to help extend battery life. Larger images of the Arduino system can be found in Appendix 2: Arduino Overview.

When building the data collection system it was essential that it be light and easily mounted to different positions on the sUAS, otherwise the weight would affect the overall balance and reduce the flying time by increasing the torque on the engine. The total weight of the Arduino package mated with the two breakout boards and LCD display is 130 grams. The cup anemometer was mounted far forward of the rotors so as to minimize vortices that could overprint the actual wind speed measurements. To accomplish this we separated the logging system from the anemometer since the logging system is where most of the weight resides and must be mounted close the main shaft. Mounting close to the main shaft allows for proper weight and balance distribution on the airframe, as weight and balance is critical to conducting a safe and stable flight, and also maximizes flight time.

### 2.3 Experimental Approach

Two experiments were conducted to test the custom wind speed payload. Experiment 1 involved an in situ comparison of the custom payload against a conventional logger/anemometer system. Experiment 2 consisted of test flights with the anemometer and MCS mounted to the sUAS. A 3 m tower with a cup anemometer was erected at the field site and a series of test flights were

performed in a broad range of wind conditions in order to determine if the wake from the sUAS affected the wind speed measurements. The stability of the sUAS was also examined during these test flights. It is important to note that the goal of these field tests was to determine that the relative accuracy of our sUAS-based wind speed measurements. This is a critical step in establishing the operational feasibility of the technique. Following the experiments, a series of flights were performed along a vertical transect in order to demonstrate the PoC.

Experiment 1 tested the custom Arduino-NovaLynx system against a Campbell Scientific datalogger (CR1000) with an RM Young 3002 anemometer. The experiment was performed outdoors with the two anemometers mounted at the same height (2 m) and separated horizontally by 1 m. The Arduino system was powered on and once a GPS lock occurred the time was copied and transferred to the Campbell Scientific datalogger. The experiment ran for 5 hours on 05 February 2013.

The field experiment, Experiment 2, was conducted at a designated RC airfield south of Coaldale, AB (**N**49° 39' 12.11", **W**112° 35' 56.26"). Data collection involved several wind events of varying magnitudes over many days. This ensured no bias conditional on the wind speed. The site is located on a broad flat plain. The vegetation consists of short grass and was surrounded by agricultural fields with low crops. Based on conventional aerodynamic roughness lengths ($z_0$) from lookup tables, we estimate the $z_0$ of the airfield to be $\approx$ 0.01 m, while the adjacent fields were between 0.03 and 0.10 m.

The custom payload was mounted to the sUAS with an extended boom created for the anemometer (Figure 2.1). Literature regarding helicopter wakes supports the placement of the anemometer and boom towards the front of the airframe (Glauert, 1935; Avissar et al., 2009).

During the second experiment, the sUAS was flown beside the 3 m tower with the RM Young 3002 anemometer mounted at the top.

While setting up both experiments the Arduino system was powered on to attain the current time in UTC from the Arduino GPS, which was displayed on the LCD. Once a GPS fix was achieved the Campbell Scientific datalogger was powered on and connected to a laptop to setup the same system time that was displayed on the Arduino. Once the system time was set the collected data could be compared in post processing. The clock was synchronized to the nearest second.

Prior to the analysis of commensurability in both experiments, the wind speed measurements were time-averaged into 5 nominal intervals: 300, 60, 40 and 30 seconds. Subsequently, the data from the Arduino/Novalynx were plotted against the reference data from the CR1000/RM Young and a linear fit was applied. The slope of the line, descriptive statistics and the $R^2$-value were used to quantify the relation.

## 2.4 Results

Results from Experiment 1 are shown in Figure 2.3, with the CR1000/RM Young data on the x-axis and the Arduino/Novalynx on the y-axis. The maximum wind speed during the experiment was 10 m/s. In all cases the relations are linear and positive. The slopes of the line equations also indicate that the relations are close to 1:1, although in all cases the CR1000/RM Young wind speed values are consistently lower than those from the Arduino/Novalynx. $R^2$-values range from 0.9366 to 0.9952 and increase (as expected) as the averaging interval increases. For all four averaging intervals these tests revealed no statistically significant difference between the CR1000/RM Young and the Arduino/Novalynx data. Collectively, these results indicate that the custom Arduino/Novalynx system is commensurate to the CR1000/RM Young system.

Results from Experiment 2 are shown in Figure 2.4. The maximum wind speed during the flights was 17 m/s. Qualitative observations indicate the sUAS remained relatively stable despite the high winds. Again, in all cases the relations are linear and positive, and the slopes between the wind speed measured from the sUAS and the tower indicate that the relation is close to 1:1. Similarly, the tower wind speed data, which was acquired with the CR1000/RM Young system, were consistently lower than those from the Arduino/Novalynx on the sUAS. The $R^2$-values are similar to those reported from the in situ testing in Experiment 1, ranging 0.943 to 0.988 and increase with increasing averaging interval. The results from paired samples t-tests indicate no statistically significant difference between the wind speed data from the sUAS and from the adjacent tower ($t = 2.429$, $df = 22$, $p = 0.02$). Thus, there does not appear to be any issues with the aircraft wake. This is consistent with literature on helicopter wakes, which shows that vortex sheet travels down, vertically from the main rotor (Glauert, 1935; Conlisk, 1997; Avissar et al., 2009). Accordingly, placement of the anemometer on the boom extending forward from the aircraft minimizes wake interference.

The PoC demonstration consisted of acquiring wind speed measurements at different altitudes with the Arduino/Novalynx payload on the sUAS. The aircraft was programmed to fly to five different altitudes, holding at each altitude for a prescribed time period (60 s) before moving onto the next. During the flight's wind speed measurements were acquired at 1 Hz. It is important to note how this approach differs from conventional wind profiling, whereby wind speed is measured simultaneously at all levels and then the data are smoothed with time-averaging before plotting. Using an sUAS it is not possible to measure wind speed simultaneously at multiple heights. Therefore, conventional wind profiling is not possible with an sUAS unless a swarm of sUASs is deployed to measure wind speed simultaneously at several heights for extended periods. For some applications where conventional techniques are difficult or unfeasible such as stack emissions, the ability to hover and measure wind speed can have important advantages.

The PoC data are shown in Figure 2.5. The vertical variation of wind speed does not conform to the typical logarithmic or power functions because the data from each altitude were acquired a few minutes apart. Instead, the data reflect the gustiness of the wind on 28 April 2013, which coincided with the passage of a cold front. The GPS data confirm that the sUAS was relatively stable in its vertical position during these flights, which is important for applications where wind speed measurements are made close to structures or natural features.

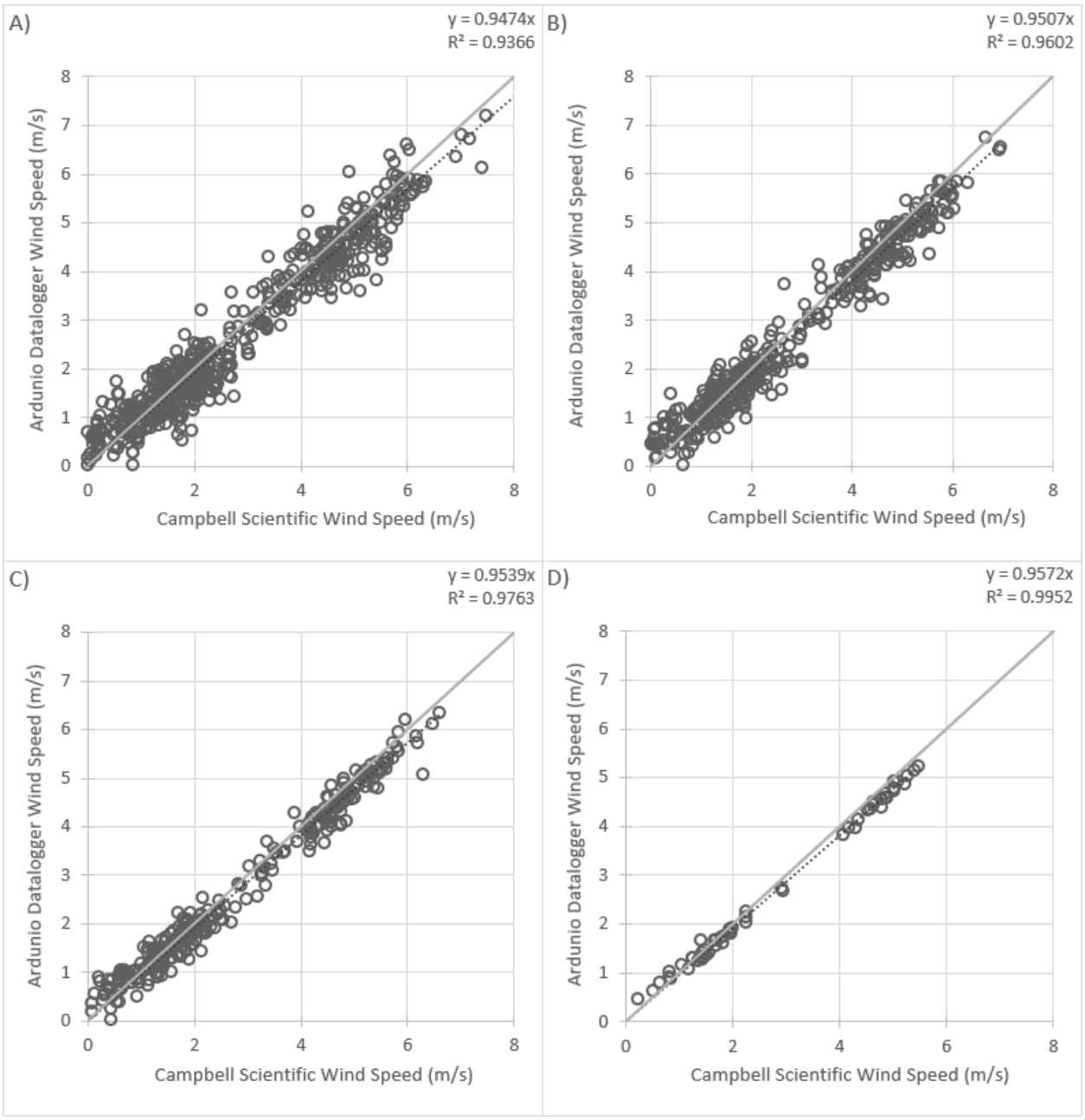


Figure 2.3 Scatterplots from Experiment 1. The averaging intervals are as follows: A) 30 s, B) 40 s, C) 60 s, D) 300 s. The line shows the 1:1 relation, while the dotted lines show the linear relation from the data.

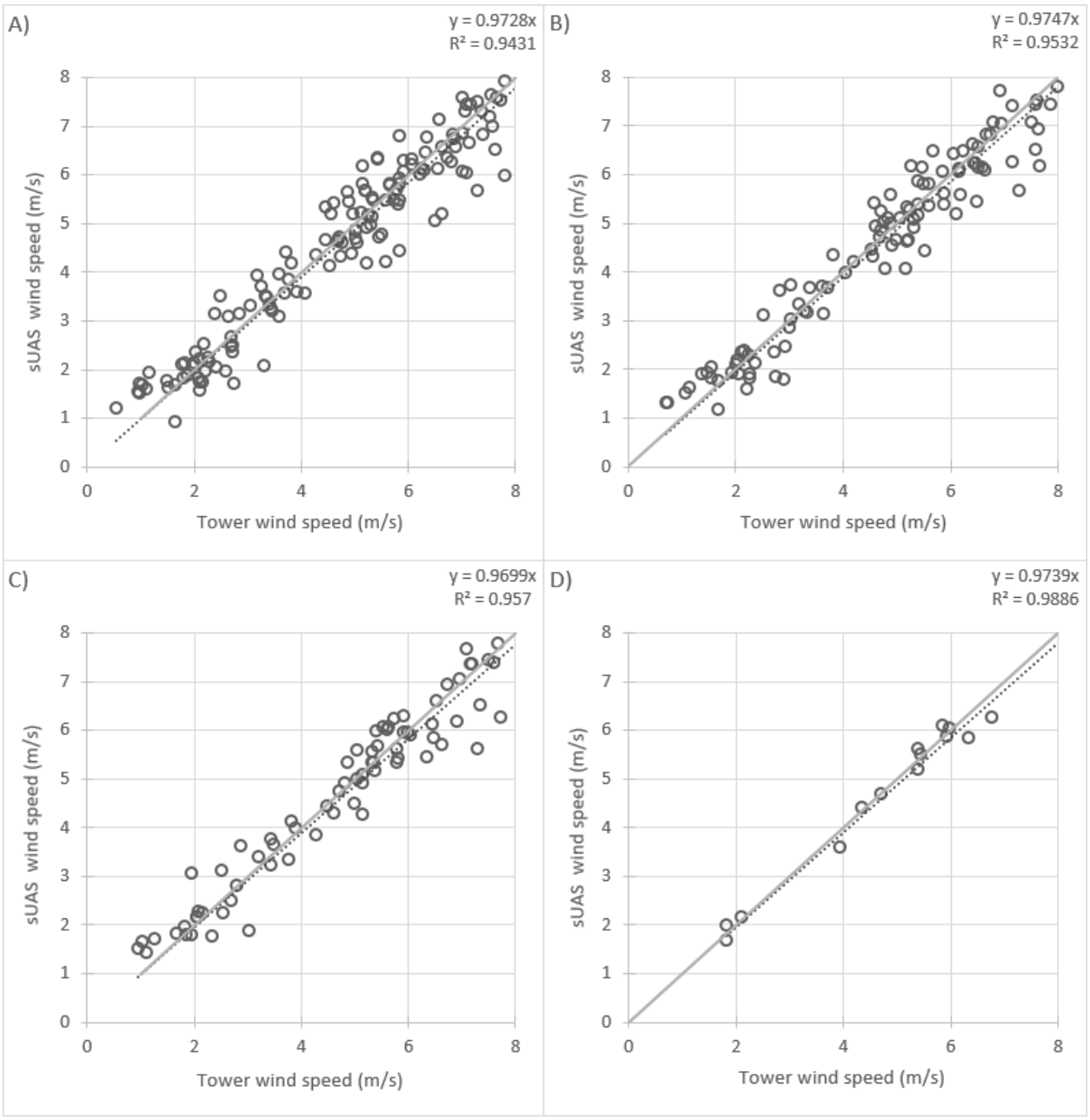


Figure 2.4. Scatterplots from Experiment 2. The averaging intervals are as follows: A) 30 s, B) 40 s, C) 60 s, D) 300 s. The solid lines show the 1:1 relation, while the dashed lines show the linear relation from the data.

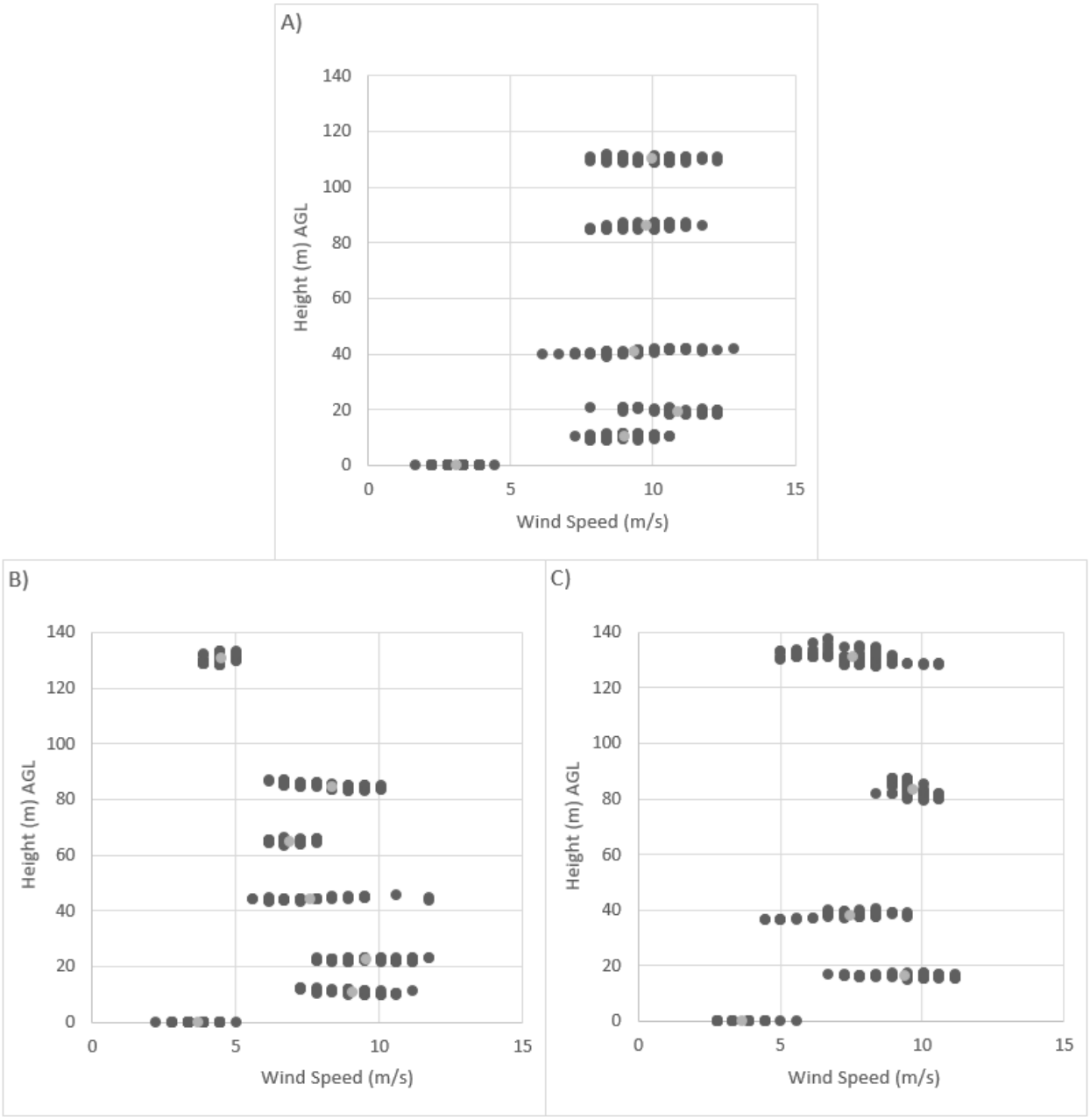


Figure 2.5. Three separate wind speed transects from the proof-of-concept flights on 28 April 2013. The light grey circles represent the median wind speed at each height above ground level (AGL), while the dark grey circles show the raw data.

## 2.5 Discussion and Conclusions

This project was structured around the design, testing and PoC demonstration of a new helicopter-based sUAS for measuring wind speed. The key measures of success are that the custom wind measurement payload developed for the sUAS is commensurate to a conventional system, and that the wake from the sUAS platform had minimal effect on the wind speed measurements. With respect to previous efforts involving sUASs for measuring wind speed, this investigation highlights some important advantages and limitations of the technique.

The relative accuracy and commensurability of the custom Arduino/Novalynx payload stands out compared to previous work, most of which has focused on the use of fixed-wing sUASs for measuring wind speed. For example, the absolute accuracy of wind speed measurements from the $M^2AV$ platform, a fixed-wing twin engine sUAS, is $\pm 1$ m/s, and the physical range is limited to 0-10 m/s (Spiess et al., 2007). In another study with the Small Unmanned Meteorological Observer (SUMO), a single engine push airplane, Kocer et al. (2011) compared SUMO measurements to a LiDAR system and found a standard uncertainty of 0.7 m/s with a confidence level of 67%. Many other studies have reported wind speed measurements from sUASs but have not clearly defined error or commensurability to other sensors (Elston et al., 2011; Bonin et al., 2012). Given the near 1:1 relation demonstrated by the Arduino/Novalynx payload relative to the CR1000/RM Young system, both during in situ testing and in flight, this research is a significant step forward in improving confidence in wind speed measurements from an sUAS.

A major limitation of the sUAS used in this research is flight time. Currently the nitro engine setup only permits roughly 10 minutes of flight time per fueling. Refueling takes only a few minutes but the requirement of monitoring fuel levels during flights reduces the simplicity the platform offers. Other power plant types such as gasoline or turbine can offer hours of flight time, which

could greatly benefit data collection at the expenses of cost. Another issue is the general wear and tear placed on the system. Throughout the study many of the high wear items including clutch, clutch-bell, starter pin, and main gear assembly needed to be replaced. Each of these items replacement required a complete disassemble of the platform. Complete teardown caused exceptional wear on the aluminum bolts, plastic pieces and other assembly parts as expense was spared in production of the hobby kit. A more robust industrial platform, which doesn't suffer from these production pitfalls, should be selected for future work. These changes should increase the flying time significantly, while also enhancing the robustness of the platform for operational use.

The sUAS platform and payload developed in this research is designed as a starting point for atmospheric research and operational applications. The expandability of the MCS provides opportunities to include other sensors, including temperature, humidity, barometric pressure, and even miniature solid state sensors for measuring atmospheric gases. Potentially the most significant use of this technology in the future is as a replacement to balloon-based sondes for atmospheric soundings. Today, very few stations in Canada conduct atmospheric soundings regularly, leading to a very sparse network of measurements. After deployment, most sondes are not retrieved, which adds to the operational cost. In the future, sUASs equipped with meteorological sensor payloads could be programmed to fly vertical transects on an operational basis, and return upon completion. One challenge for this type of approach is the UAS regulations, which typically restrict the flying altitude; however, this may change once the competency of the technology and operators is demonstrated.

## 2.6 References


Avissar, R., Holder, H. E., Abehserra, N., Bolch, M. A., Canning, P., Magalhaes, J., . . . Prince, K. (2009). The Duke University helicopter observation platform. *Bulletin of the American Meteorological Society, 90*(7), 939-954.

Bonin, T., Chilson, P., Zielke, B., & Fedorovich, E. (2013). Observations of the Early Evening Boundary-Layer Transition Using a Small Unmanned Aerial System. (0006-8314). Retrieved 2013/01/01, from Springer Netherlands http://dx.doi.org/10.1007/s10546-012-9760-3

Bonin, T., Chilson, P., Zielke, B., Klein, P. , & Leeman, J. (2012). Development and comparisons of wind retrieval algorithms for small unmanned aerial systems. *Geoscientific Instrumentation, Methods and Data Systems Discussions, 2*, 953-979.

Conlisk, A. T. (1997). Modern helicopter aerodynamics. *Annual review of fluid mechanics, 29*(1), 515-567.

Corrigan, C. E., Roberts, G. C., Ramana, M. V., Kim, D., & Ramanathan, V. (2008). Capturing vertical profiles of aerosols and black carbon over the Indian Ocean using autonomous unmanned aerial vehicles. *Atmospheric Chemistry and Physics, 8*(3), 737-747.

Daida, J. M., Russell, P. B., Crawford, T. L., & Vesecky, J. F. (1994, 8-12 Aug. 1994). *An unmanned aircraft vehicle system for boundary-layer flux measurements over forest canopies.* Paper presented at the Geoscience and Remote Sensing Symposium, 1994. IGARSS '94. Surface and Atmospheric Remote Sensing: Technologies, Data Analysis and Interpretation., International.

Egger, J., Bajrachaya, S., Egger, U., Heinrich, R., Reuder, J., Shayka, P., . . . Wirth, V. (2000). Diurnal Winds in the Himalayan Kali Gandaki Valley. Part I: Observations. *Monthly Weather Review, 128*(4), 1106-1122.

Elston, J. S., Roadman, J., Stachura, M., Argrow, B., Houston, A., & Frew, E. (2011). The tempest unmanned aircraft system for in situ observations of tornadic supercells: design and VORTEX2 flight results. *Journal of Field Robotics, 28*(4), 461-483.

Frew, E. W., Elston, J., Argrow, B., Houston, A., & Rasmussen, E. (2012). Sampling Severe Local Storms and Related Phenomena: Using Unmanned Aircraft Systems. *Robotics & Automation Magazine, IEEE, 19*(1), 85-95.

Giebel, G., U., Schmidt P., Bange, J., La Cour-Harbo, A., Reuder, J., Mayer, S., . . . Mølgaard, J. (2012). Autonomous Aerial Sensors for Wind Power Meteorology-A Pre-Project: Danmarks Tekniske Universitet, Risø Nationallaboratoriet for Bæredygtig Energi.

Glauert, H. (1935). Airplane propellers *Aerodynamic theory* (pp. 169-360): Springer.

Holland, G. J., McGeer, T., & Youngren, H. (1992). Autonomous Aerosondes for Economical Atmospheric Soundings Anywhere on the Globe. *Bulletin of the American Meteorological Society, 73*(12), 1987-1998.

Holland, G. J., Webster, P. J., Curry, J. A., Tyrell, G., Gauntlett, D., Brett, G., . . . Vaglienti, W. (2001). The Aerosonde Robotic Aircraft: A New Paradigm for Environmental Observations. *Bulletin of the American Meteorological Society, 82*(5), 889-901.

Kocer, G, Mansour, M, Chokani, N, Abhari, RS, & Müller, M. (2011). Full-Scale Wind Turbine Near-Wake Measurements Using an Instrumented Uninhabited Aerial Vehicle. *Journal of solar energy engineering, 133*(4).

Koçer, G. (2012). *Full-scale wind turbine flow field measurements using an instrumented uninhabited aerial vehicle.* Diss., Eidgenössische Technische Hochschule ETH Zürich, Nr. 20660, 2012.

Lin, P. H., & Lee, C. S. (2008). The eyewall-penetration reconnaissance observation of Typhoon Longwang (2005) with unmanned aerial vehicle, Aerosonde. *Journal of Atmospheric and Oceanic Technology, 25*(1), 15-25.

Reuder, J., Brisset, P., Jonassen, M., Muller, M., & Mayer, S. (2009). The small unmanned meteorological observer SUMO: a new tool for atmospheric boundary layer research. . *Meteorologische Zeitschrift 18*, 141-147.

Reuder, J., Brisset, P., Jonassen, M., Müller, M., & Mayer, S. (2008). SUMO: A small unmanned meteorological observer for atmospheric boundary layer research. *IOP Conference Series: Earth and Environmental Science, 1*(1), 012014.

Reuder, J., Jonassen, M. O., & Ólafsson, H. (2012). The Small Unmanned Meteorological Observer SUMO: Recent developments and applications of a micro-UAS for atmospheric boundary layer research. *Acta Geophysica, 60*(5), 1454-1473.

Sotelino, L. G., De Coster, N., Beirinckx, P., & Peeters, P. (2012). *Intercomparison of cup anemometer and sonic anemometers on site at Uccle/Belgium.* Paper presented at the WMO Technical Conference on Meteorological and Environmental Instruments and Methods of Observation (TECO-2012).

Spiess, T., Bange, J., Buschmann, M., & Vörsmann, P. (2007). First application of the meteorological Mini-UAV 'M2AV'. *Meteorologische Zeitschrift, 16*(2), 159-169.

Thomas, R. M., Lehmann, K., Nguyen, H., Jackson, D. L., Wolfe, D., & Ramanathan, V. (2011). Measurement of turbulent water vapor fluxes using a lightweight unmanned aerial vehicle system. *Atmospheric Measurement Techniques Discussions, 4*(4), 5529-5568.

van den Kroonenberg, A., Martin, T., Buschmann, M., Bange, J., & Vörsmann, P. (2008). Measuring the Wind Vector Using the Autonomous Mini Aerial Vehicle M2AV. *Journal of Atmospheric and Oceanic Technology, 25*(11), 1969-1982.

van den Kroonenberg, A., Spieß, T., Buschmann, M., Martin, T., Anderson, P. S., Beyrich, F., & Bange, J. (2007). Boundary layer measurements with the autonomous mini-UAV M 2 AV. *Proceedings of DACH2007, Hamburg, Germany*, 10-14.

# CHAPTER 3: BOUNDARY-LAYER MEASUREMENTS OF PARTICULATE MATTER WITH A SMALL AUTONOMOUS HELICOPTER: PROOF OF CONCEPT

## 3 Abstract

This chapter reports the design and performance of a new airborne system for measuring particulate matter (PM) in the atmospheric boundary layer. The system comprises a small unmanned aircraft system (sUAS) and a payload for measuring PM concentration. The integration of these technologies was motivated by the gap between satellite-based measurements which yield PM data at relatively coarse spatial scales, ground or tower-based methods which have limited mobility and spatial coverage, and airborne methods which are either expensive or require manual operation. The research was structured in 2 phases. Phase 1 involved the design and testing of a miniature PM measurement payload, comprising a PM sensor, a measurement and control system (MCS), and a GPS receiver for recording the x, y, and z coordinates of each measurement. Phase 2 involved (a) field testing to determine if the aircraft had any effect on the accuracy of PM measurements, and (b) Proof-of-Concept (PoC) demonstration, whereby the sUAS and PM payload were used to measure vertical variations of PM concentration and flux. One of the goals of phase 1 was to design an inexpensive and lightweight PM payload that was commensurate to other commonly used sensors, and could be mounted on a wide range of sUASs. To meet this goal, the payload was initially designed with a lightweight commodity sensor (Sharp GP2Y1010AU0F), but controlled tests indicated that the Sharp is not commensurable to the reference PM sensor (TSI DustTrak, model 8520). The following limitations of the Sharp sensor were noted: (i) incommensurability between multiple Sharp sensors, (ii) the requirement of time-averaging to filter variability in the signal, (iii) inconsistent response over a range of PM levels relative to the DustTrak, thus precluding calibration relative to a reference sensors, and (iv) a saturation effect at PM levels that might occur in real

applications. Therefore, the Sharp was abandoned in favor of the DustTrak, and the sUAS used in phase 2 was tailored to carry the heavier DustTrak. The latter was secured to an Align T-Rex 700 nitro-powered helicopter equipped with a DJI Ace Waypoint autopilot system. The DustTrak intake was mounted to a boom extending beyond the reach of the main rotor at the front of the aircraft. Field tests showed strong agreement between PM measurements from the DustTrak on the sUAS, versus those from a second DustTrak mounted to a tower at the same height above the ground. For the PoC, the sUAS acquired measurements of PM concentration and wind speed along vertical profiles, thus providing the ability to resolve PM concentration and horizontal PM flux at different positions above the surface. Overall, this project demonstrates the technical challenges and opportunities for measuring PM with a helicopter sUAS.

## 3.0 Introduction

Particulate matter (PM) is an important atmospheric constituent and plays a key role in a number of climate processes and air quality issues (Anenberg et al., 2010; Buseck, 2010; Silva et al., 2013). PM can be made up of many different constituents, either natural or manmade, such as dust, soot and sea salt. PM smaller than 10 μm ($PM_{10}$) represents a significant health concern because upon inhalation these particles are able to penetrate into the alveolar region of the lungs (Costa et al., 1997; Bickis, 1998; Anenberg et al., 2010; Silva et al., 2013). PM also affects Earth's radiation budget with allied impacts on global climate (Twomey, 1977; Albrecht, 1989; Pósfai et al., 2010). At local to regional scales PM can impact ecosystems by depositing pollutants (Addison et al., 1980; Barrie et al., 1980; Seaward, 1993; Kelly et al., 2009; Timoney et al., 2009; Mitchell et al., 2010). In some regions, climate change and a growing anthropogenic footprint may be altering, if not abruptly increasing, the emission and atmospheric concentration of particulates like dust (Neff et al., 2008; Mahowald et al., 2010; Kan et al., 2012), while in other regions there is evidence of a decrease in PM and related particulates (e.g., Environmental Protection Agency, 2011; Fox et al., 2012). Our ability

to measure PM is important, therefore, in order to understand the broad range of geophysical, biophysical and anthropogenic processes that release it to the atmosphere, and thus understand its fate in terrestrial and aquatic ecosystems.

Many different measurement techniques have been developed in an attempt to better understand the atmospheric processes involving PM. In general, there are two scales of measurement for operational monitoring of PM. For regional to global coverage, satellite systems are typically used, such as Moderate Resolution Imaging Spectroradiometer (MODIS) and the Geostationary Operational Environmental Satellite (GOES). These and other sensors can measure the aerosol optical depth (AOD), which is the degree to which aerosols prevent the transmission of light by absorption or scattering. Because AOD is related to PM, the latter can be estimated empirically from satellite data. One of the issues with satellite-derived measurements of PM is that the spatial resolution is very coarse; often one value is used to represent relatively large areas (e.g. several $km^2$). On the other side of the scale is a group of operational measurement techniques involving instruments deployed on the ground, on towers or on airborne platforms. This group involves passive collectors and active sensors. Most of the sensors in this group collect measurements of PM at a point on or near the ground surface. Examples of instruments in this group include low cost passive collectors such as scanning electron microscope stubs or UNC sampler, (e.g., Wagner et al., 2001; Harner et al., 2006) Polyurethane foam (PUF) disks, (e.g., Maricq et al., 2004), dichotomous virtual impactors, (e.g., Solomon et al., 1983) and active sensors TEOM (e.g., Allen et al., 1997); GRIMM (e.g., Peters et al., 2006); DustTrak (e.g., Kingham et al., 2006); MetOne (e.g., Zhu et al., 2007). In these cases, the unit of measure varies from PM mass to PM concentration. Ground-based remote sensing measurements of PM, including those from light detection and ranging (LiDAR) systems (e.g., Collis, 1966), can be used to extend the vertical reach of surface networks and can operate in continuous mode, but these systems are fixed and therefore

only measure PM directly overhead. Mobile LiDAR systems can overcome their in situ counterparts (e.g., Raut et al., 2009), but they are expensive and the spatial extent of surveys is limited by road access.

Airborne techniques that complement and enhance ground-based PM measurement systems can involve manned aircraft, sondes, tethered balloons and kites equipped with PM sensors (Daniels, 1989; Mcgowan et al., 1996; Walesby et al., 2010; Reiche et al., 2012). Radiosondes are a commonly used technique for airborne measurements. Sondes are able to measure a range of atmospheric parameters with dynamic measurement payloads (Hirono et al., 1976; Hooper et al., 1986; Ferrare et al., 1995). Radiosondes are also cheaper and safer than manned aircraft, and can stay aloft in excess of two hours, ascend to over 35 km, and travel more than 300 km away from their release point (NOAA, 2013). An issue with the radiosonde platform is that they travel with the winds aloft, which could move the platform away from the particular area under research. Manned aircraft also offer excellent platforms for atmospheric studies. They allow for large payloads with controlled visits to the area or event under scrutiny (Wandinger et al., 2002). They are however very expensive to operate and maintain, and due to this reason, are outside the budgets of many scientific research groups. Kites and tethered balloons are practical for a number of reasons. They can carry large payloads, up to several kilograms. They are also capable of long-duration PM measurement at a single point in the atmosphere, and at high altitude (~ 500 m). They can measure vertical profiles and can also be controlled. However, kites have one important drawback – they require a certain level of wind speed to generate lift, e.g., > 4 m $s^{-1}$ (McGowan et al., 2008). For this, and perhaps other reasons, aircraft are not routinely used for PM measurements.

In order to extend the vertical reach of ground-based atmospheric measurement networks, and to complement existing airborne platforms, several research programs have tested sUASs

equipped with custom payloads, particularly within the last 5-10 years (Ramana et al., 2007; van den Kroonenberg et al., 2007; Martin et al., 2010; Mayer et al., 2010; Am et al., 2011; Cook et al., 2012). For the purpose of this paper, the term "small" refers to UASs that are portable and generally weigh less than 10 kg. These platforms are considerably less expensive to purchase and operate compared to piloted aircraft and LiDAR systems, making them highly accessible for research applications, and viable for routine operations like regulatory auditing. They also offer greater flexibility, reduced risk compared to manned aircraft, and autonomous operation. sUASs have already been used to measure a range of variables in the ABL (Daida et al., 1994; Lin et al., 2008; McGonigle et al., 2008; Roberts et al., 2008; Martin et al., 2010; McGill et al., 2011; Cook et al., 2012; Frew et al., 2012; Kroonenberg et al., 2012; Bonin et al., 2013). To date, most research with sUASs has focused on fixed-wing platforms, which requires continuous movement. For some applications, however, it may be preferable to maintain a fixed position for extended periods, such as stack emission monitoring in situations where the operation and maneuverability of a fixed wing sUAS may be too risky due to terrain or infrastructure.

The purpose of this study was to design and test a small, autonomous sUAS for measuring PM in the atmospheric boundary layer. To extend previous research using fixed wing sUASs, the main focus of this research was a vertical take-off and landing (VTOL, a.k.a. helicopter) sUAS, which offers greater maneuverability and control. The research was structured in 2 phases: (1) design and testing of a custom PM measurement payload and (2) field testing and PoC demonstration. The initial payload design was influenced by the payload weight restriction of most small VTOLSs (e.g. Aeryon Scout, ~300 g), and the potential compatibility issues with a broad range of autopilot systems. Most PM sensors currently used for ground-based measurements are too bulky for sUASs, and they do not easily allow for synchronization with GPS receivers, which are needed to link PM measurements to x, y, z coordinates for real-world applications. Therefore, in phase 1 the research

focused on developing a self-contained, lightweight, custom payload with its own measurement and control system (MCS), GPS and PM sensor. A key indicator of the performance of the custom payload was its commensurability relative to other widely used PM sensors. For this assessment a TSI DustTrak (model 8520) PM sensor served as the reference. In phase 2 the PM measurement payload was secured to an sUAS and flown next to a tower, also equipped with the same PM sensor, to determine if the aircraft had any effects on the measurements. Finally, the PoC was demonstrated by using the sUAS and DustTrak to acquire vertical measurements of PM concentration and flux.

### 3.1 Background: PM measurement and commodity sensors

A common thread underpinning many ground-based PM measurement networks is the use of optical light scattering technology to determine the concentration of aerosols. This principle is used in many professional-grade sensors (e.g., TSI, MetOne, GRIMM), as well as many commodity sensors (e.g., Shinyei, Sharp, Dylos Corp.). The latter group is far less expensive than the former, by up to several orders of magnitude, but is relatively unproven in terms of their commensurability with the professional-grade sensors. Some of key differences between these groups of sensors are: i) the method of measuring the aerosols, ii) the method of drawing the sample through the sensor, and iii) the type of light source. More expensive sensors either partially sample the aerosol stream, which allows higher accuracy (e.g., nephelometer), or use whole stream testing, which ultimately is less accurate (opacity). More expensive sensors also typically use a pump to draw air into the sensor and the light source is coherent (laser), whereas the low-cost commodity sensors typically are passive with respect to air intake and measure the drop in voltage cause by particulates as they pass by an LED light source.

Owing to their low cost, commodity PM sensors are beginning to gain popularity as part of portable air quality sensing systems (Budde et al., 2012; Budde et al., 2013; Devarakonda et al.,

2013), and community-led air quality sensing networks e.g., (KickStarter, 2012; William, 2013). By definition, commodity sensors are affordable and easy to obtain. The original (intended) use of the commodity PM sensors is for air purifiers and air cleaners, but they are now seeing greater use outdoors. These sensors use light scattering with an LED light source and inexpensive circuitry, which results in prices generally below $25.00 USD. The absence of a pump means that commodity PM sensors either use a hole in the sensor to capture ambient air as it passes by, or they use a heating element to push ambient air past the sensor.

Some of the features that make commodity sensors particularly attractive in the context of sUASs include their small size, light weight, and low power requirements. In contrast, the intake pumps and lasers in the more expensive PM sensors result in much higher power requirements and overall size of the instruments, which results in larger batteries and higher weight. As a general rule of thumb, larger payloads require larger sUASs. Based on these issues, the commodity sensors are an attractive alternative for sUASs. The question, however, is whether they are equivalent to the more expensive sensors used in air quality research and monitoring. To date, commodity sensors have not been extensively tested.

### 3.2 Methodology

The organization of research outlined in this chapter is similar to that presented in Chapter 2: 1) sensor testing and 2) field testing and PoC demonstration. However, instead of simply attaching a conventional PM measurement system to an sUAS, we first attempted to make the PM payload as light as possible, thus making it compatible with the widest possible range of sUASs, many of which have exceedingly small payload capacities (e.g., < 300 g). It was also important that each PM measurement coincided with a real-world x, y, z coordinate, as measured by a GPS. Therefore, the payload needed to support both a GPS receiver and a PM sensor, and the two instruments needed

to be compatible with the MCS. Most professional grade PM instruments are not designed to integrate with a GPS, but by taking advantage of the analog output signal from TSI's DustTrak (model 8520), which is a heavy (> 1500 g) yet robust instrument widely used for PM measurements, it was possible to measure PM simultaneously from the Sharp and DustTrak using the MCS, thus establishing whether the commodity sensor was commensurate with the professional-grade sensor. In phase 2, the PM measurement payload was secured to an sUAS and field tests were conducted to verify the PM measurements against a reference sensor mounted to a 3 m tower, and to demonstrate the PoC.

### 3.2.1 Phase 1: Commodity Sensor Testing

There are many lightweight PM sensors available on the market, but the design of the Sharp GP2Y1010 (Osaka, Japan) is more suitable than others to our research needs due to its large opening, which allows particles to easily pass through the light beam and exit the rear of the sensor body (Fig. 3.1), and its fast response (0.28 ms). Other commodity sensors, like the Shinyei PPD42NS (Kobe, Japan), do not allow free passage of PM through the sensor, and also have much slower response (e.g., 30 s). In some regards, the Sharp sensor is similar to the DustTrak in that the measured dust concentration is proportional to the output voltage. Both use an analog method that incorporates a photometer, which quantifies the overall level of light scattering, which is then converted to PM concentration in mg $m^{-3}$. Furthermore, it is possible to connect a tube to the DustTrak and run it directly to the opening on the Sharp, thus ensuring the 2 sensors measure the same air during testing.

Figure 3.1. An image of the Sharp GP2Y1010 sensor showing the sensor hole (centre of enclosure) and interface connection pins.

The Sharp GP2Y1010 is an analog sensor that outputs a voltage measured on an analog input. It uses an infrared emitting diode and phototransistor, diagonally arranged, to detect PM in air. Light reflects off the particles passing through the hole and are picked up by the photodiode, which is transformed into a voltage. The voltage needs to be amplified to read the change. The analog voltage output signal from the Sharp phototransistor has been empirically-related to PM concentration by the manufacturer. In the reference manual for the sensor, it is stated that the GP2Y1010 has a sensitivity range of 0.3 to 0.65 volts for a change in PM mass concentration of 100 μg $m^{-3}$ (SHARP, 2006). According to the manufacturer's specifications, the conversion of voltage to PM mass concentration (in mg $m^{-3}$) is linear in the range from 0 to 530 μg $m^{-3}$. Based on the manufacturer's specifications (TSI, 2010), the equation to convert voltage ($V$) to PM concentration ($C_s$) in μg $m^{-3}$ is approximately as follows:

$$C_s = \frac{(V-0.5803)}{5.817} \times 1000 \qquad \text{[Eq. 3.1]}$$

The measurement and control system (MCS) used to operate the Sharp and measure its voltage was an Arduino Mega 2560 microcontroller. The Arduino platform is an open-source electronics tool based on flexible, easy-to-use hardware and software. Arduino boards are designed to combine with many different sensors and integrate in specific ways through computer code in the Arduino Integrated Development Environment. The microcontroller on the Arduino board is programmed using the Arduino programming language, which is based on the Wiring language. Processor, memory, and connection requirements for the datalogger were taken into consideration when choosing an appropriate Arduino board. Clock speeds and memory were also taken into consideration as an increase in both can provide fast, continuous data acquisition. An added circuit is required for the LED input terminal between the Arduino and Sharp sensor. The added circuit requires a 150 Ohm resistor and a 220 μF capacitor (Figure 3.2).

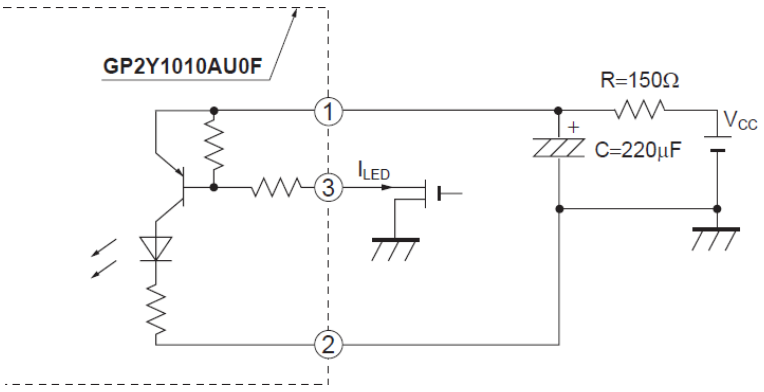


Figure 3.2. Circuit diagram for the LED input terminal (SHARP, 2006)

The first step in designing the sUAS payload was to determine if the Sharp was commensurate with other, more widely used PM sensors. For this purpose we chose a DustTrak aerosol monitor (model 8520), which is widely used in ground-based air quality research and monitoring (e.g., Etyemezian et al., 2004; Kingham et al., 2006). Due to its size (221 x 150 x 87 mm), power

requirements, and overall and weight (2.0 kg with battery), the DustTrak is incompatible with most small VTOL UASs, so initially it was used as a reference to gauge the commensurability of the Sharp. It uses a 90º light scattering laser diode to determine mass concentration. Aerosol samples are drawn into the measurement chamber using an air pump. The air sample is then illuminated with laser light. Particles in the sample scatter light in all directions. A lens 90º to both the aerosol stream and laser beam collects and focuses this scattered light onto a photodetector, which converts the light into a voltage. The DustTrak has a resolution of 1.0 μg $m^{-3}$ and can measure up to 100,000 μg $m^{-3}$.

The DustTrak is also capable of outputting an analog voltage (0 to 5 VDC), which makes it directly compatible with the Arduino Mega MCS. The analog function on the DustTrak is accessed through a mini-DIN interface cable that connects to the rear of the device. The analog output has 4 user-selectable output scaling ranges: 0 to 100,000 μg $m^{-3}$, 0 to 10,000 μg $m^{-3}$, 0 to 1,000 μg $m^{-3}$ and 0 to 100 μg $m^{-3}$. These ranges are set in the DustTrak software. Depending on the environment being sampled, the scaling should be selected according to the anticipated range of PM concentrations. By using the analog-to-digital (A/D) converter on the Arduino Mega, the ability to resolve PM concentration is controlled by 2 parameters: the scaling range, and the bit resolution of A/D converter on the MCS, which is 10-bit (or 1024 different values). According to the manufacturer's specifications, the following equations are used to establish the PM resolution per A/D bit (Eq. 3.2), PM concentration per output voltage (Eq. 3.3) and the output voltage per A/D bit (Eq. 3.4):

$$\frac{DustTrak\ Monitor\ Scaling\ Range}{Bits\ of\ Resolution} = \frac{1.0\ mg/m^3}{1024\ bits} = 0.00097\ \frac{mg/m^3}{bit}\ OR\ 0.97\ \frac{\mu g/m^3}{bit} \quad \text{[Eq. 3.2]}$$

$$\frac{DustTrak\ Monitor\ Scaling\ Range}{Full\ Scale\ Voltage} = \frac{1.0\ mg/m^3}{5\ volts} = 0.02\ \frac{mg/m^3}{volt}\ OR\ 20\ \frac{\mu g/m^3}{volt} \quad \text{[Eq. 3.3]}$$

$$\frac{Full\ Scale\ Voltage}{Bits\ of\ Resolution} = \frac{5\ VDC}{1024\ bits} = 0.00488\ \frac{VDC}{bit} \quad \text{[Eq. 3.4]}$$

### 3.2.2 Controlled tests and results

Four controlled tests were performed in order to test the Sharp sensor and determine commensurability relative to the DustTrak (Table 3.1). The tests cover a broad range, from low (ambient) to high concentration. For the latter, solder smoke was used to increase PM levels from ambient to high concentration. Prior to starting the experiments, the commensurability of three Sharp GP2Y1010 sensors was tested. This was done to determine if the Sharp sensors performed consistently. In all subsequent tests one Sharp sensor was compared to the DustTrak. The main details of the experiments are presented in Table. 3.1.

A small hose was connected from the DustTrak intake directly to the opening on the Sharp sensor in order to ensure the calibrated reference device and the Sharp sensors measured the same air during the tests (Fig. 3.3). By activating the pump on the DustTrak, the air was drawn directly through both sensors at the standard flow rate setting of 1.7 L/min.

Table 3-1 Overview of controlled tests.

| Experiment | Sensor | Frequency | Duration | Statistics |
|---|---|---|---|---|
| **A:** Comparison of 3 different Sharp sensors base levels. (*Means were compared)* | 3 Sharps | 1 Hz | 50 min. | 1st Mean: 3.3 $\mu g \cdot m^{-3}$<br>2nd Mean:16.0 $\mu g \cdot m^{-3}$<br>3rd Mean: 19.1 $\mu g \cdot m^{-3}$ |
| **B:** Indoor ambient PM comparison | DustTrak | 1 Hz | 55 min. | Mean: 9.8 $\mu g \cdot m^{-3}$<br>SD: 6.74 $\mu g \cdot m^{-3}$ |
| | Sharp | | | Mean: 12.17 $\mu g \cdot m^{-3}$<br>SD: 6.77 $\mu g \cdot m^{-3}$ |
| **C:** Indoor moderate PM comparison | DustTrak | 1 Hz | 1 h 34 min. | Mean: 6.35 $\mu g \cdot m^{-3}$<br>SD: 12.99 $\mu g \cdot m^{-3}$ |
| | Sharp | | | Mean: 12.44 $\mu g \cdot m^{-3}$<br>SD: 8.87 $\mu g \cdot m^{-3}$ |
| **D:** Indoor high PM comparison | DustTrak | 1 Hz | 13 min. | Not Applicable |
| | Sharp | | | Not Applicable |

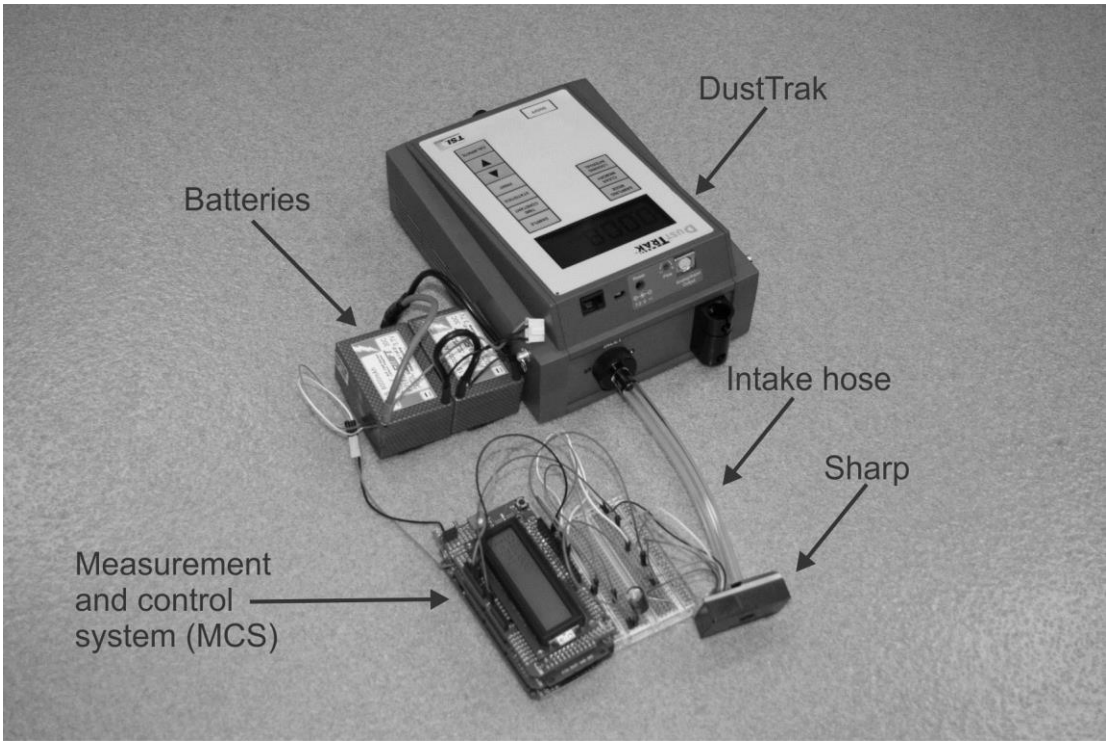


Figure 3.3. The experimental setup for testing commensurability between the Sharp and DustTrak.

**Experiment A:**

Experiment A compared 3 different Sharp GP2Y1010 sensors. Each sensor was placed in a fume hood for 50 minutes to record a base reading. The experiments were conducted in sequence and the measurements were averaged for a period of 30 seconds. The results are shown in Figure 3.4. Means from the 3 sensors ranged from 3.3 μg $m^{-3}$ to 19.1 μg $m^{-3}$. These base readings differed by up to 15.8 μg $m^{-3}$ between the lowest mean to the highest and the closest two sensors differed by 3.1 μg $m^{-3}$. These results show large variability within these sensors, which is mostly likely attributed to the intrinsic error of the sensors.

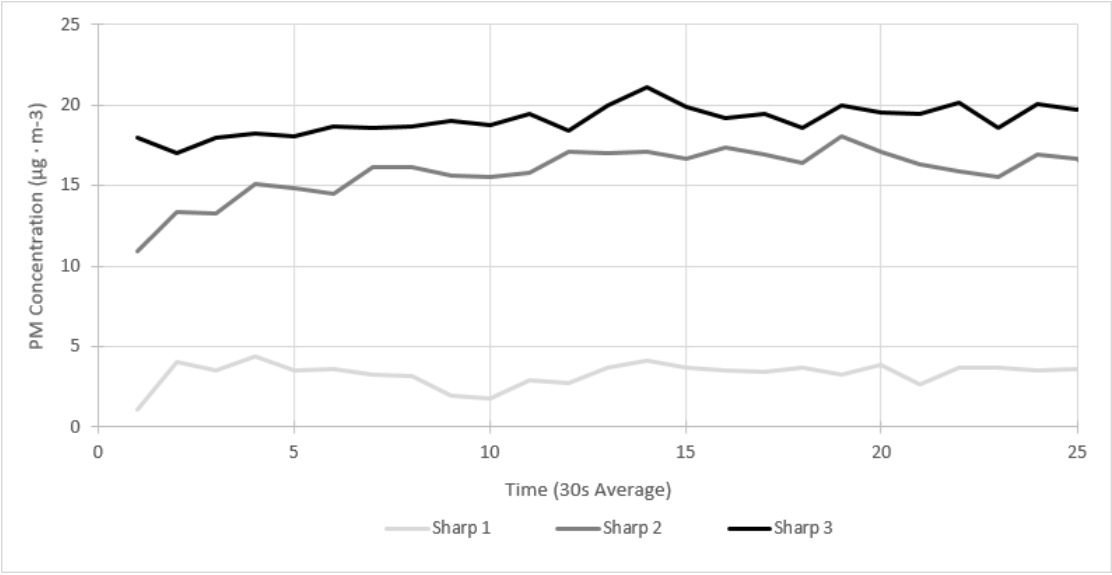


Figure 3.4. Comparison of three different Sharp commodity sensors base readings. Values shown above have been averaged over 30 second period.

**Experiment B:**

Experiment B compared PM measurements between the DustTrak and Sharp sensors at ambient PM concentrations in a fume hood while the fan circulated. The graph in Figure 3.5A shows that the Sharp's raw (1 Hz) signal was much more variable that the DustTrak's during the experiment. At times, the values from the Sharp were negative, which is due to the voltage reading falling below the zero level. These readings are believed to be caused by internal noise within the sensor, or noise in the analog reading. The downward trend of the DustTrak is interpreted as a progressive lowering of the ambient PM concentration within the room due to the operation of the fume hood. There are some spikes in the DustTrak measurements, which may be the results dust released by other activities occurring in the lab during the measurement period (e.g., handling of soil samples).

Budde et al. (2012) suggested that a 30-minute averaging period may be required for the Sharp sensor to be comparable to the DustTraks, however, this is impractical for PM measurements with sUASs since it would not even result in one value per flight on most battery-operated VTOLs.

Scatterplots found in Figure 3.5A and B demonstrate the difference in sensor noise and reading performance. Figure 3.5A displays the raw data of both sensors. The DustTrak sensor readings display a narrow band in a negative trend. The Sharp's raw data points display a wide disordered band with no trend, signifying greater noise in the sensor. Figure 3.5B displays a 1:1 scatterplot directly comparing the relationship between the two sensors, no correlation was observed.

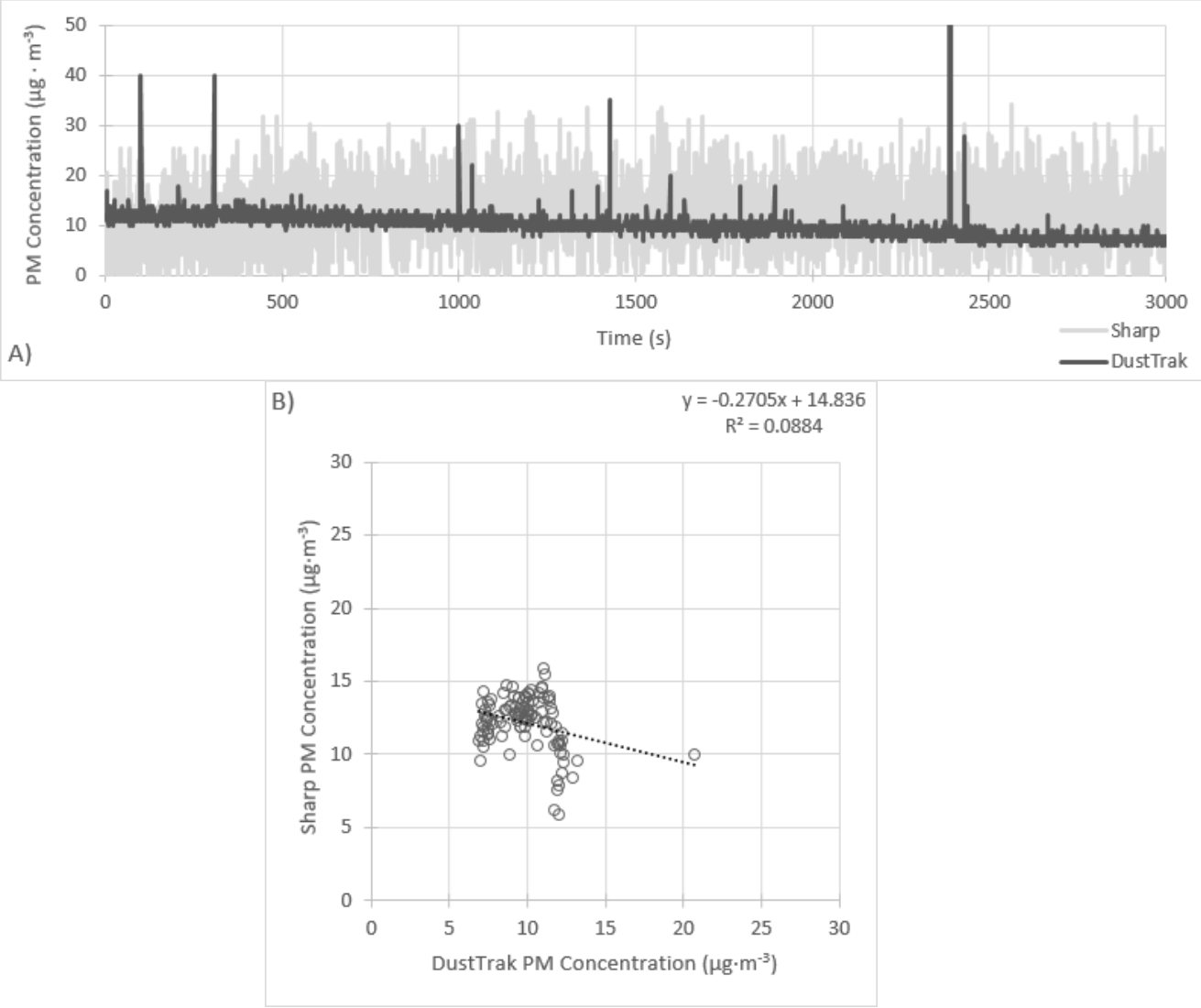


Figure 3.5. A comparison of the Sharp vs. DustTrak during experiment B. A) Shows the raw (1 Hz) data, while B) shows a 1:1 comparison of the data from both sensors after 30 second time-averaging, no correlation was observed.

**Experiment C:**

Experiment C consisted of measurements during moderate PM concentration. The PM was generated by pouring sand into a large plastic box containing both PM sensors, and then closing the lid. Dust released by this process was measured by the sensors. This procedure resulted in elevated PM levels initially, followed by a tapering effect as the dust particles settled. Graphs in Figure 3.6A, B show both the raw and averaged measurements from each sensor compared using a 1:1 scatterplot, no correlation is observed. Compared to the DustTrak, the Sharp did not capture the same peaks in PM concentration at the beginning of the experiment and failed to capture the tapering effect. This is shown in Figure 3.6C. After 30-second time-averaging, the Sharp's PM measurements are almost three times higher than the DustTrak, and still displayed greater variability.

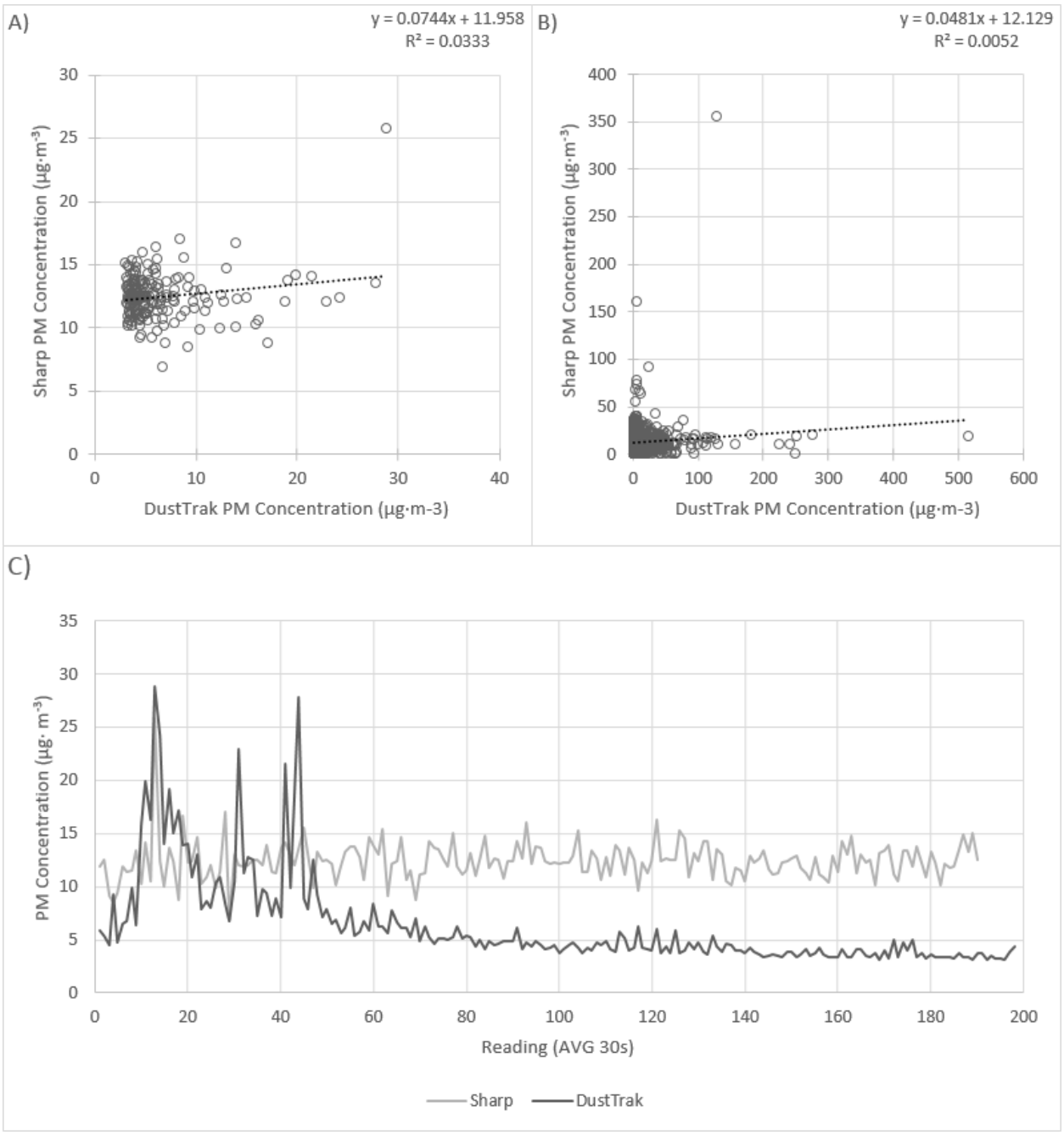


Figure 3.6 A) 1:1 scatterplot comparison of the Sharp vs. DustTrak during experiment C using the raw (1 Hz) data from the DustTrak and Sharp, respectively, while B) shows the data from both sensors after 30 second time-averaging. C) Displays the averaged 30 second data for both sensors.

**Experiment D:**

Experiment D was conducted to test the Sharp against the DustTrak under very high PM concentrations. During the experiment PM was generated with solder smoke, which was released

into a sealed box containing both sensors. While the PM concentration produced during the experiment is not realistic under most natural conditions, the experiment does reveal an important limitation of the Sharp sensor. Figure 3.7A shows the time series of the raw (1 Hz) measurements for the full duration of the experiment; it shows that the response of the sensors is very different. This difference is believed to be due to the sampling methods used by each sensor. The DustTrak uses an active vacuum system to sample the air, while the Sharp uses a passive system, which only perceives the PM that floats by. With these differences the DustTrak has a higher probability of accurately quantifying the air quality versus the Sharp but slightly lags due to the speed in which the vacuum pump is sampling.

While the DustTrak was able to measure up to 38,290 μg $m^{-3}$ the Sharp saturated at 526.7 μg $m^{-3}$. This effect is also shown by the plateau in the time series for the Sharp sensor in Figure 3.7B. Therefore, for some air quality applications the Sharp will be unable to measure the PM concentration. This could be problematic in some regions, like China, where the PM concentration can greatly exceed the Sharp's saturation limit (e.g., up to 1,000 μg $m^{-3}$ as measured in Harbin, China, in October 2013).

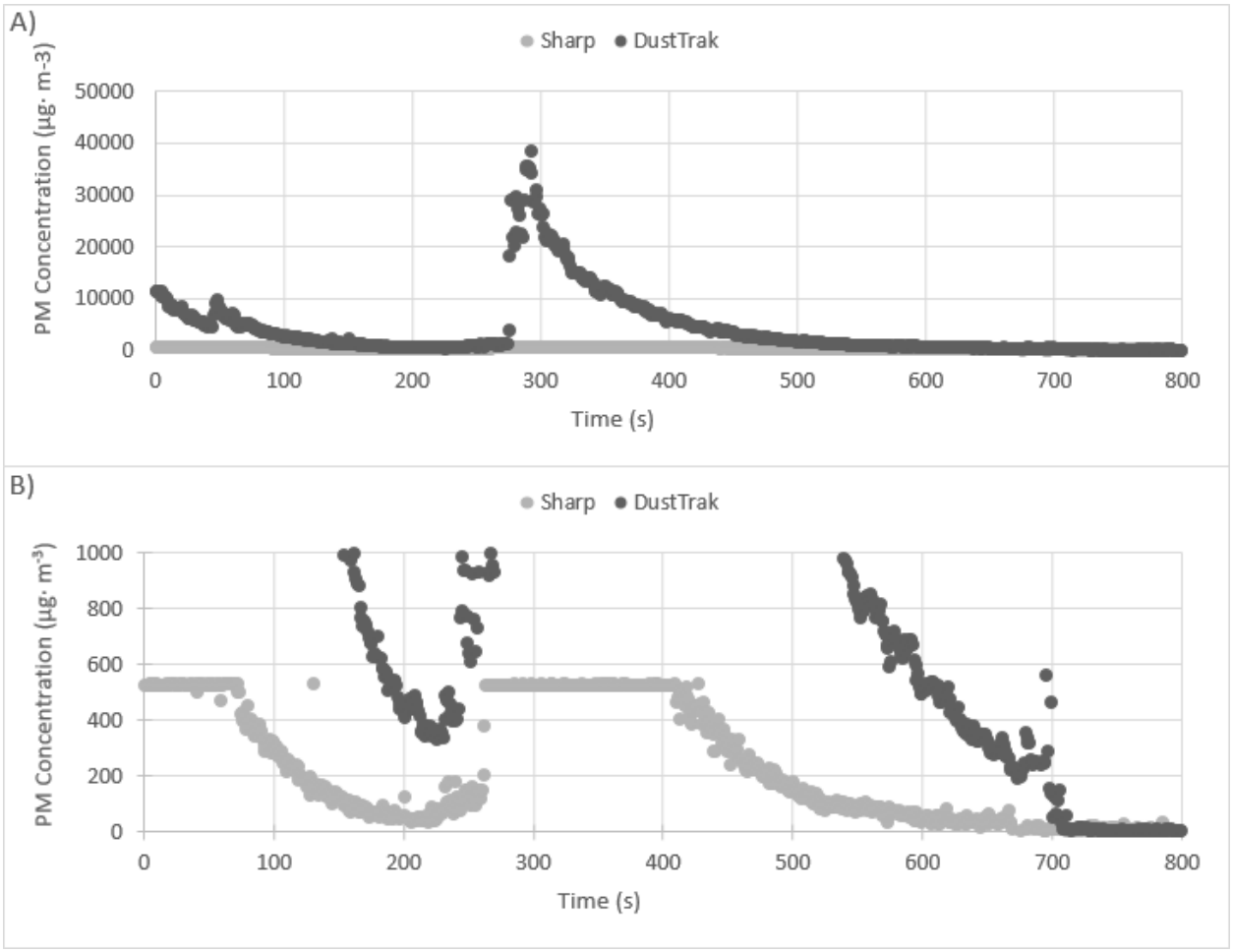

Figure 3.7. Comparison of the Sharp vs. DustTrak during experiment D. A) Shows the full time series, while B) shows zoomed in portion of the full time series.

### 3.2.3 Synthesis of test results

A summary of the commensurability of the Sharp and DustTrak sensors is presented in Figure 3.8. In order for the two sensors to be commensurable there should be a well-defined relation. However, the wide scatter indicates they are not commensurable, and that there is no way of calibrating the Sharp relative to the DustTrak.

In addition to the lack of commensurability with respect to the DustTrak, the following limitations of the Sharp were noted from the experiments: First, there is a large discrepancy between different Sharp sensors according to Experiment A. This signifies the requirement of developing a

custom calibration for each Sharp sensor. Second, according to experiment B, the Sharp signal is very noisy and requires significant time averaging to smooth the data. Third, the relation between the Sharp and DustTrak is inconsistent, which means the former cannot be calibrated relative to the latter. Fourth, the Sharp's saturation limit restricts its use to low PM concentrations. Overall, according to the results of the controlled experiments, it was not possible to develop a reliable and accurate PM measurement payload based on the Sharp. Therefore, for Phase 2 the sUAS was based on the design limitations imposed by the heavier DustTrak.

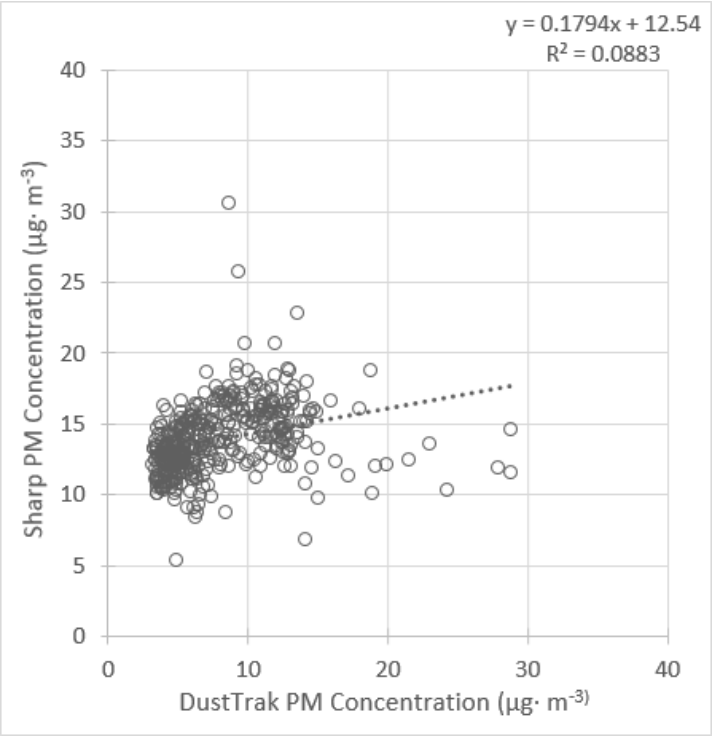


Figure 3.8. A 1:1 scatterplot of PM concentration from the Sharp and DustTrak for Experiments B, C and D (30-second data). The DustTrak is plotted on the x-axis and the Sharp on the y-axis.

### 3.2.4 Phase 2: Field testing and proof-of-concept

#### 3.2.4.1 sUAS design

In order to support the weight of the DustTrak PM sensor (2.0 kg), we developed a custom sUAS from a hobbyist nitro-powered VTOL (Align T-Rex 700N, ALIGN, Taiwan) and a DJI Ace Waypoint autopilot system (Figure 3.9) (DJI, Hong Kong, China). The 700N is a flybarless (a two-

bladed rotor system that does not have a flybar to help stabilize) 7-channel helicopter system with a 1562 mm main rotor diameter and a tail rotor diameter of 281 mm. The rigid frame design is built with carbon fiber and the helicopter is powered by a .91 cu. in. nitro engine producing roughly 4 HP. The empty weight of the aircraft is 4.1 kg and the total length is 1.335 m. The DustTrak was attached to the skids under the sUAS using four attachment points built into the DustTrak casing. A sampling tube that connects to the DustTrak's vacuum pump was affixed to a boom that projected forward beyond the reach of the rotor blades (Figure 3.9). The traditional helicopter platform was an excellent choice for this experiment as adding elements to the frame of the helicopter didn't affect flight performance due to the robustness and flight characteristics of this design. Maximum payload weight is not known, but the helicopter was been successfully tested up to 12 kg.

The DJI AceOne autopilot system used for this project is specially designed for a traditional helicopter platform. The complete autopilot system is under 150 g and allows for multiple flight-control modes. The system was used in conjunction with a DJI Ground Control Station (GCS), which allows for flight tracking and updating during the mission. Mission parameters were programmed into the GCS and uploaded to the sUAS platform via telemetry link.

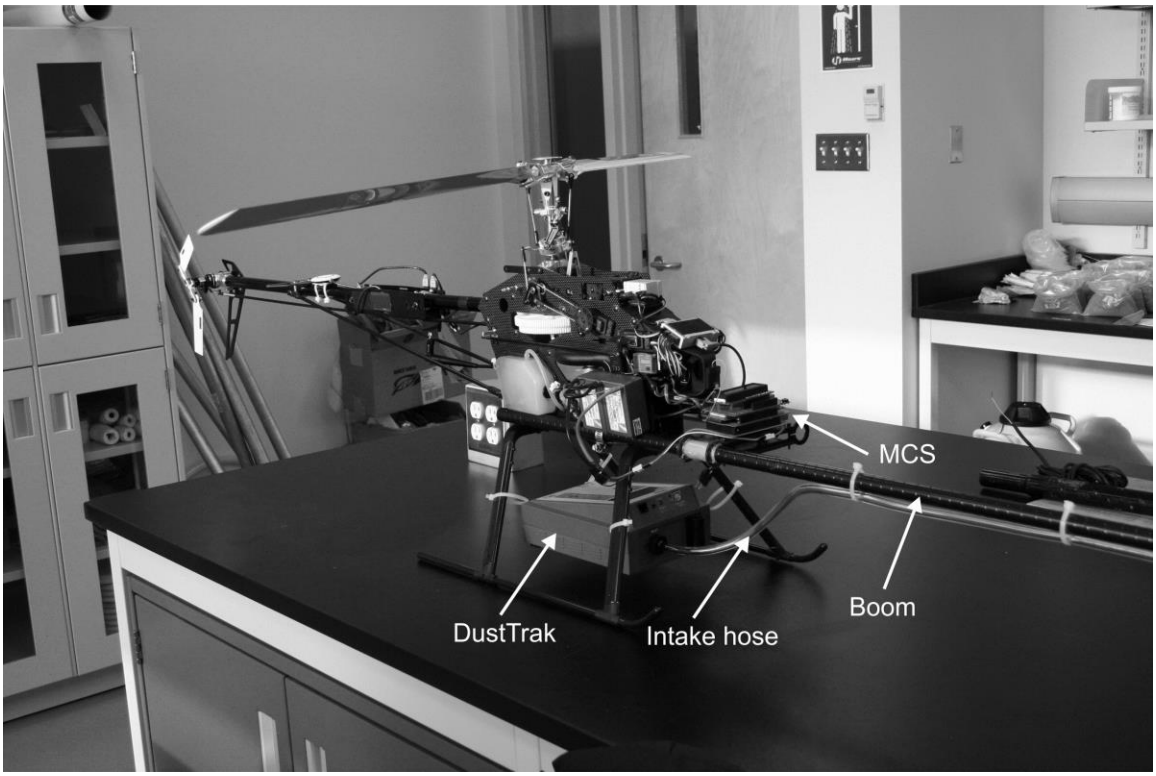


Figure 3.9. The T-Rex 700N with the DustTrak secured to the landing gear and the boom extending to the right of the image. The MCS is also indicated.

#### 3.2.4.2 Field experiment and demonstration

Initial testing followed by PoC demonstration was carried out at a field site near Coaldale, AB. The testing was done to ensure the in-flight PM measurements from the sUAS were unaffected by the aircraft, and therefore equivalent to PM measurements made in situ. This was accomplished by erecting a 3 m tower at the field site, and affixing a second DustTrak to it, which served as the reference PM measurement. During test flights, the sUAS hovered at 3 m above the surface and approximately 4 m north of the tower. Flights were performed on October 4 and 22 of 2013. On all occasions the wind was westerly; therefore, it is assumed that the two DustTraks were sampling approximately equivalent PM concentration. For the PoC demonstration an anemometer was attached to the sUAS and the aircraft was flown at three elevation intervals above the surface while collecting wind speed and PM concentration, thus providing a measure of horizontal PM flux.

Figure 3.10 displays raw data collected by both DustTrak devices on October 22, 2013. The recorded ambient PM values appear to be similar with related trends. Further evaluation of these results was conducted by averaging the values over a 30 second time period (Figure 3.10C). Averaged plots helped to remove discrepancies between DustTrak measurements due to their positional difference. To examine whether there was a statistically significant difference between the two DustTraks an independent samples t-test was used. The test results indicate no statistically significant difference between the two devices ($t = 1.194$, $df = 3424$, $p = .233$). The means and standard deviations of the two sensors were very similar: sUAS DustTrak (mean = 16.57, SD = 4.27) versus the tower DustTrak (mean = 16.74, SD = 4.39). Based on these findings, it appears that the PM measurements from the sUAS and tower were comparable; therefore, when the aircraft is facing into the wind, it has minimal effect on the measurement of PMs.

In preparation for the PoC demonstration the sUAS was pre-programmed to fly to three different heights above the ground surface (20, 90 and 140 m), hover in place for 90 seconds, then land. The wind speed and direction during the flight was 5.5 $ms^{-1}$ and 280°, respectively. Results showed the highest levels of PM concentration were recorded at 90 meters and 20 meters.

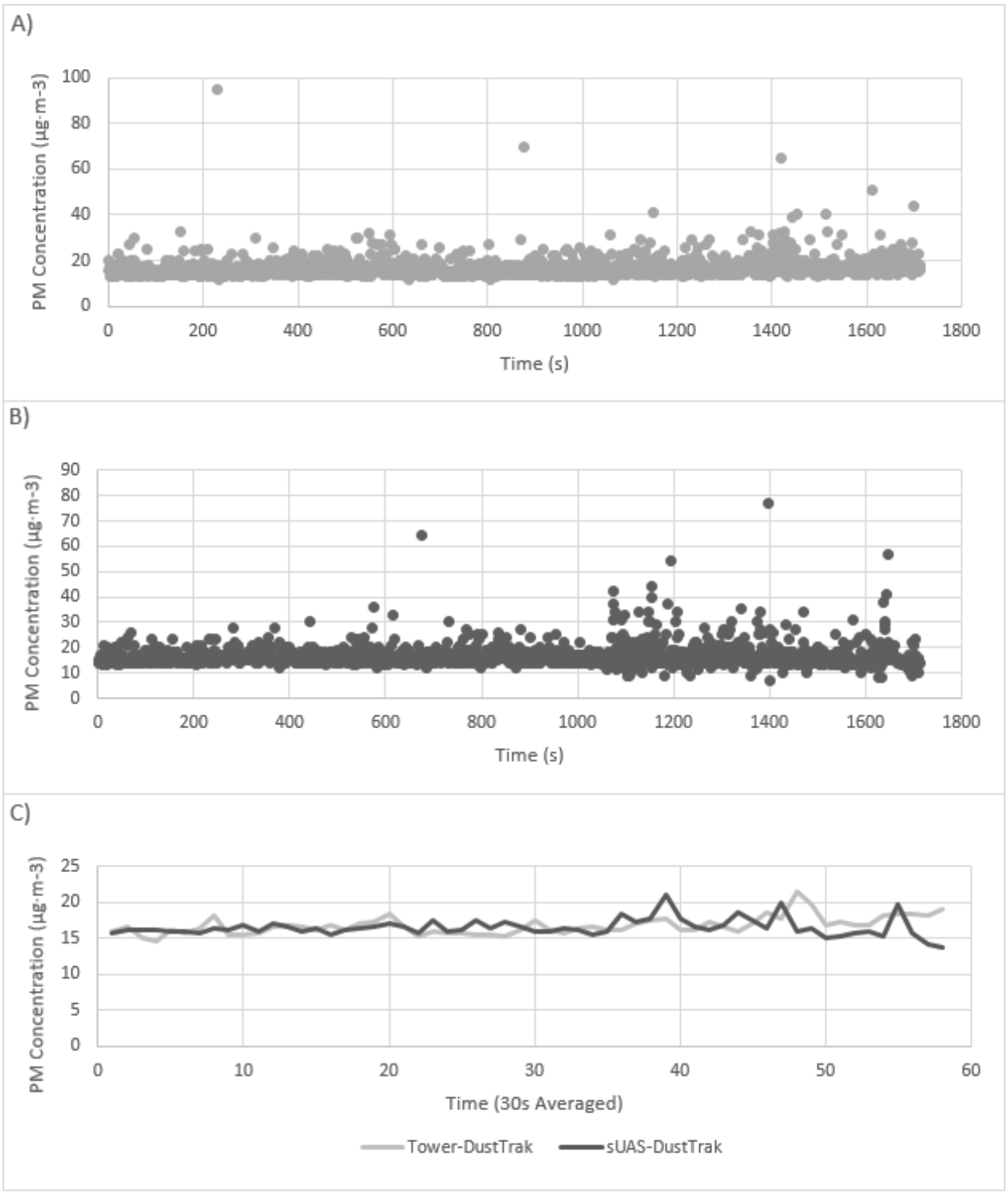


Figure 3.10. Comparison of in situ and sUAS DustTrak systems while sampling ambient aerosols readings over three different flights. The sUAS mounted DustTrak is shown in A) and Tower mounted DustTrak is shown in B). Plot C) is a time averaged comparison of DustTrak systems.

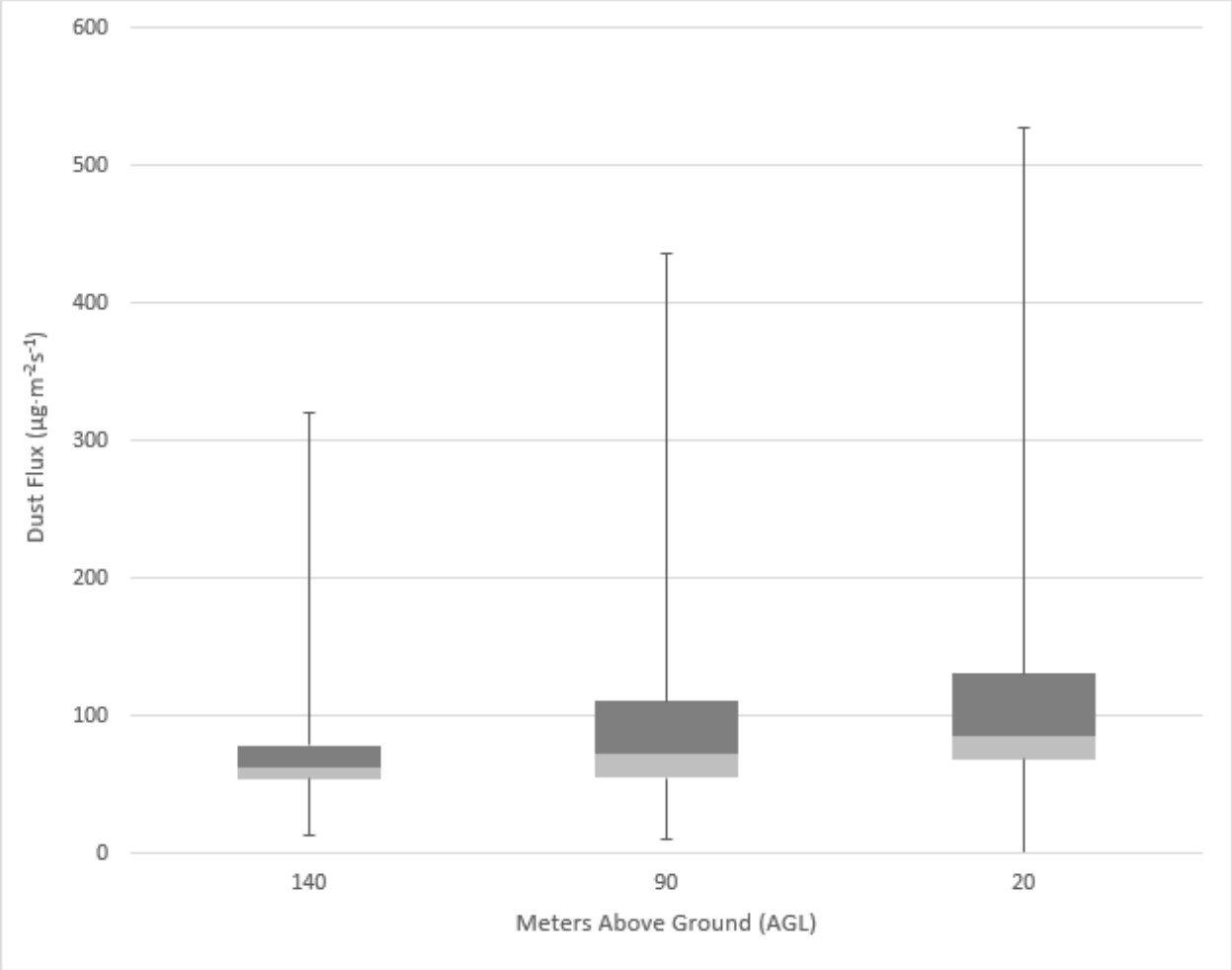


Figure 3.11. Calculated dust flux ($\mu g \cdot m^{-2} \cdot s^{-1}$) at different altitudes using the PM concentration measured $\mu g \cdot m^{-3}$ and wind speed measured in $m \cdot s^{-1}$ at altitude. Box plot depicts lower and upper extremes, lower and upper quartiles, and medians.

### 3.3 Discussion and conclusions

This study has exposed some of the challenges and opportunities related to acquiring airborne measurements of PM with a VTOL-based sUAS platform. In this regard, a key challenge in developing any form of atmospheric measurement payload for an sUAS is to ensure the measurements are commensurate with existing sensors, and that the aircraft does not affect the accuracy of the measurements. Without commensurability, PM measurements from sUASs are only useful in a relative sense, and therefore not generally suitable to real applications like regulatory auditing, environmental monitoring, or air quality model testing. However, due to payload weight restrictions, the task of transferring ground-based sensors to sUASs is not straightforward. Few ground-based PM sensors are small enough for sUASs, and most lack the ability to integrate directly with peripheral MCSs and GPS receivers. The latter is especially important for resolving spatial variations of PM concentration, which is an important limitation of existing ground-based PM measurement techniques.

Phase 1 of this research was motivated by the need to develop a lightweight PM measurement payload that could integrate with a wide array of sUASs, including many with very small payload weight restrictions (e.g. Aeryon Scout, ~300 g). However, the test results demonstrate that the Sharp commodity PM sensor is not commensurable to the more widely used DustTrak sensor. Indeed, the Sharp sensor is not the only small-scale PM sensor available, but its design is better suited than others to sUAS applications. Furthermore, it is being used in many portable devices and air quality monitoring networks (Reggente et al., 2010; Budde et al., 2012; Budde et al., 2013; Devarakonda et al., 2013). Several key issues with the Sharp sensor were identified. These issues could potentially restrict its usefulness in environmental research and include variations in the performance of one Sharp sensor to another, the need to time-average measurements to filter noise, and a low saturation limit. Due to these issues, the goal of developing a lightweight PM payload based on the Sharp

sensor was not achieved. Consequently, rather than designing the payload based on the sUAS weight restriction, the research shifted so that the payload determined the sUAS design.

In Phase 2, the VTOL sUAS was developed to carry the DustTrak sensor. Accordingly, the sUAS was based on a VTOL platform that could support the weight of the DustTrak. Field tests with a collocated tower showed a near 1:1 relation between the DustTrak PM measurements onboard the sUAS during hover, versus those from a second DustTrak at the same height on the tower. This confirms that the aircraft has little to no effect on the PM measurements during hover. For the PoC demonstration the sUAS and DustTrak measured vertical variations of PM mass concentration, and with the addition of an anemometer, the PM flux was determined. Therefore, this research demonstrates that it is possible to collect spatial measurements of airborne PM levels with an sUAS and PM sensor.

This research highlights some of the advantages for measuring PM in the atmospheric boundary layer with a VTOL sUAS. The ability to pre-program coordinates and maintain hover, as shown in the PoC demonstration, is ideally suited to a range of applications and settings where other techniques may be too cumbersome to operate. For example, industrial stack-emissions are monitored for regulatory compliance, environmental impact assessments, abatement performance, and process control. A VTOL sUAS with a PM measurement payload can hover in place at a pre-defined position above or near the stack to measure PM mass concentration and flux (if equipped with an anemometer). Few techniques can satisfy this safely.

This research also highlights some notable limitations of the system we developed. One of the main limitations is the relatively short flying time, presumably due to the added weight of the DustTrak. The longest flight was 8 minutes, which affords a rather limited spatial coverage for resolving spatial variations of PM either in the vertical or horizontal directions. The flying time may

be extended significantly by changing the nitro engine to a gas-turbine engine, but this was beyond the scope of this research. Second, the configuration of the intake hose on the boom extending out in front of the aircraft requires that it is always facing into the wind. If the aircraft faces away from the wind, it will measure PM from its own exhaust. Applying a heading hold in the autopilot software is the only way to ensure the boom faces the wind; however, manual intervention is required if the wind direction changes during a flight. Third, regulations in Canada dictate that sUAS flights are restricted to the lower part of the atmospheric boundary layer (e.g., < 150 m). Flights higher up in the boundary layer may be granted, however, after competency is demonstrated.

Despite some limitations, there are opportunities to build on the research presented in this chapter. Of paramount importance is the miniaturization of PM sensors. Lightweight, robust and high quality PM sensors that can integrate with MCSs and GPS receivers will be extremely valuable for moving from PoC towards operational implementation. The number of sUASs that can carry PM measurement payloads will expand considerably if the weight is kept to a minimum. For now, the PM sensors dictate the sUAS required to carry them.

## 3.4 References


Addison, P. A., & Puckett, K. J. (1980). Deposition of atmospheric pollutants as measured by lichen element content in the Athabasca oil sands area. *Canadian Journal of Botany, 58*(22), 2323-2334.

Albrecht, B. A. (1989). Aerosols, cloud microphysics, and fractional cloudiness. *Science, 245*(4923), 1227-1230.

Allen, G., Sioutas, C., Koutrakis, P., Reiss, R., Lurmann, F. W., & Roberts, P. T. (1997). Evaluation of the TEOM® method for measurement of ambient particulate mass in urban areas. *Journal of the Air & Waste Management Association, 47*(6), 682-689.

Am, C., Jihoon, K., Sanghyo, L., & Changdon, K. (2011). Wind Estimation and Airspeed Calibration using a UAV with a Single-Antenna GPS Receiver and Pitot Tube. *Aerospace and Electronic Systems, IEEE Transactions on, 47*(1), 109-117.

Anenberg, S. C., Horowitz, L. W., Tong, D. Q., & West, J. J. (2010). An estimate of the global burden of anthropogenic ozone and fine particulate matter on premature human mortality using atmospheric modeling. *Environmental Health Perspectives, 118*(9), 1189.

Barrie, L. A., & Kovalick, J. (1980). *A Wintertime Investigation of the Deposition of Pollutants Around an Isolated Power Plant in Northern Alberta*: Alberta Environment.

Bickis, U. (1998). Hazard prevention and control in the work environment: airborne dust. *World Health, 13*, 16.

Bonin, T., Chilson, P., Zielke, B., & Fedorovich, E. (2013). Observations of the Early Evening Boundary-Layer Transition Using a Small Unmanned Aerial System. (0006-8314). Retrieved 2013/01/01, from Springer Netherlands http://dx.doi.org/10.1007/s10546-012-9760-3

Budde, M., Barbera, P., El Masri, R., Riedel, T., & Beigl, M. (2013). *Retrofitting smartphones to be used as particulate matter dosimeters.* Paper presented at the Proceedings of the 17th annual international symposium on International symposium on wearable computers.

Budde, M., Busse, M., & Beigl, M. (2012). *Investigating the use of commodity dust sensors for the embedded measurement of particulate matter.* Paper presented at the Networked Sensing Systems (INSS), 2012 Ninth International Conference on.

Buseck, P. R. (2010). Atmospheric-Particle Research: Past, Present, and Future. *Elements, 6*(4), 208-209.

Collis, R. T. H. (1966). Lidar: a new atmospheric probe. *Quarterly Journal of the Royal Meteorological Society, 92*(392), 220-230.

Cook, D. E., Strong, P. A., Garrett, S. A., & Marshall, R. E. (2012). A small unmanned aerial system (UAS) for coastal atmospheric research: preliminary results from New Zealand. *Journal of the Royal Society of New Zealand, 43*(2), 1-8.

Costa, D. L., & Dreher, K. L. (1997). Bioavailable transition metals in particulate matter mediate cardiopulmonary injury in healthy and compromised animal models. *Environmental health perspectives, 105*(Suppl 5), 1053.

Daida, J. M., Russell, P. B., Crawford, T. L., & Vesecky, J. F. (1994, 8-12 Aug. 1994). *An unmanned aircraft vehicle system for boundary-layer flux measurements over forest canopies.* Paper presented at the Geoscience and Remote Sensing Symposium, 1994. IGARSS '94. Surface and Atmospheric Remote Sensing: Technologies, Data Analysis and Interpretation., International.

Daniels, A. (1989). Measurements of atmospheric sea salt concentrations in Hawaii using a Tala kite. *Tellus B, 41*(2), 196-206.

Devarakonda, S., Sevusu, P., Liu, H., Liu, R., Iftode, L., & Nath, B. (2013). *Real-time air quality monitoring through mobile sensing in metropolitan areas.* Paper presented at the Proceedings of the 2nd ACM SIGKDD International Workshop on Urban Computing.

Environmental Protection Agency, EPA. (2011). Our Nation's Air: Status and Trends Through 2010 (U. S. E. P. Agency, Trans.) (pp. 27). Research Triangle Park , North Carolina.

Etyemezian, V., Ahonen, S., Nikolic, D., Gillies, J., Kuhns, H., Gillette, D., & Veranth, J. (2004). Deposition and removal of fugitive dust in the arid southwestern United States: Measurements and model results. *Journal of the Air & Waste Management Association, 54*(9), 1099-1111.

Ferrare, R. A., Melfi, S. H., Whiteman, D. N., Evans, K. D., Schmidlin, F. J., & Starr, D. O'C. (1995). A comparison of water vapor measurements made by Raman lidar and radiosondes. *Journal of Atmospheric and Oceanic Technology, 12*(6), 1177-1195.

Fox, T. A., Barchyn, T. E., & Hugenholtz, C. H. (2012). Successes of soil conservation in the Canadian Prairies highlighted by a historical decline in blowing dust. *Environmental Research Letters, 7*(1), 014008.

Frew, E. W., Elston, J., Argrow, B., Houston, A., & Rasmussen, E. (2012). Sampling Severe Local Storms and Related Phenomena: Using Unmanned Aircraft Systems. *Robotics & Automation Magazine, IEEE, 19*(1), 85-95.

Harner, T., Pozo, K., Gouin, T., Macdonald, A. M., Hung, H., Cainey, J., & Peters, A. (2006). Global pilot study for persistent organic pollutants (POPs) using PUF disk passive air samplers. *Environmental Pollution, 144*(2), 445-452.

Hirono, M., Fujiwara, M., & Itabe, T. (1976). Behavior of the stratospheric aerosols inferred from laser radar and small ion radiosonde observations. *Journal of Geophysical Research, 81*(9), 1593-1600.

Hooper, W. P., & Eloranta, E. W. (1986). Lidar measurements of wind in the planetary boundary layer: the method, accuracy and results from joint measurements with radiosonde and kytoon. *Journal of climate and applied meteorology, 25*(7), 990-1001.

Kan, H., Chen, R., & Tong, S. (2012). Ambient air pollution, climate change, and population health in China. *Environ Int, 42*, 10-19.

Kelly, E. N., Short, J. W., Schindler, D. W., Hodson, P. V., Ma, M., Kwan, A. K., & Fortin, B. L. (2009). Oil sands development contributes polycyclic aromatic compounds to the Athabasca River and its tributaries. *Proc Natl Acad Sci U S A, 106*(52), 22346-22351.

KickStarter, Air Quality Egg -. (2012). Air Quality Egg. Retrieved 11/12/2013, 2013, from http://www.kickstarter.com/projects/edborden/air-quality-egg

Kingham, S., Durand, M., Aberkane, T., Harrison, J., Gaines Wilson, J., & Epton, M. (2006). Winter comparison of TEOM, MiniVol and DustTrak PM< sub> 10</sub> monitors in a woodsmoke environment. *Atmospheric Environment, 40*(2), 338-347.

Kroonenberg, A. C., Martin, S., Beyrich, F., & Bange, J. (2012). Spatially-Averaged Temperature Structure Parameter Over a Heterogeneous Surface Measured by an Unmanned Aerial Vehicle. *Boundary-Layer Meteorology, 142*(1), 55-77.

Lin, P. H., & Lee, C. S. (2008). The eyewall-penetration reconnaissance observation of Typhoon Longwang (2005) with unmanned aerial vehicle, Aerosonde. *Journal of Atmospheric and Oceanic Technology, 25*(1), 15-25.

Mahowald, N. M., Kloster, S., Engelstaedter, S., Moore, J. K., Mukhopadhyay, S., McConnell, J. R., . . . Curran, M. A. J. (2010). Observed 20th century desert dust variability: impact on climate and biogeochemistry. *Atmospheric Chemistry and Physics, 10*(22), 10875-10893.

Maricq, M. M., & Xu, N. (2004). The effective density and fractal dimension of soot particles from premixed flames and motor vehicle exhaust. *Journal of Aerosol Science, 35*(10), 1251-1274.

Martin, S., Bange, J., & Beyrich, F. (2010). Meteorological profiling of the lower troposphere using the research UAV "M2AV Carolo". *Atmos. Meas. Tech. Discuss., 3*(6), 5179-5209.

Mayer, S., Sandvik, A., Jonassen, M. O., & Reuder, J. (2010). Atmospheric profiling with the UAS SUMO: a new perspective for the evaluation of fine-scale atmospheric models. *Meteorology and Atmospheric Physics, 116*(1-2), 15-26.

McGill, P. R., Reisenbichler, K. R., Etchemendy, S. A., Dawe, T. C., & Hobson, B. W. (2011). Aerial surveys and tagging of free-drifting icebergs using an unmanned aerial vehicle (UAV). *Deep Sea Research Part II: Topical Studies in Oceanography, 58*(11-12), 1318-1326.

McGonigle, A. J. S., Aiuppa, A., Giudice, G., Tamburello, G., Hodson, A. J., & Gurrieri, S. (2008). Unmanned aerial vehicle measurements of volcanic carbon dioxide fluxes. *Geophysical Research Letters, 35*(6), L06303.

McGowan, H. A., & Clark, A. (2008). A vertical profile of PM10 dust concentrations measured during a regional dust event identified by MODIS Terra, western Queensland, Australia. *Journal of Geophysical Research: Earth Surface (2003–2012), 113*(F2).

Mcgowan, H. A., & Sturman, A. P. (1996). A kite based atmospheric sounding system. *Boundary-Layer Meteorology, 77*(3-4), 395-399.

Mitchell, R., Maher, B. A., & Kinnersley, R. (2010). Rates of particulate pollution deposition onto leaf surfaces: temporal and inter-species magnetic analyses. *Environ Pollut, 158*(5), 1472-1478.

Neff, J. C., Ballantyne, A. P., Farmer, G. L., Mahowald, N. M., Conroy, J. L., Landry, C. C., . . . Reynolds, R. L. (2008). Increasing eolian dust deposition in the western United States linked to human activity. *Nature Geoscience, 1*(3), 189-195.

NOAA. (2013). NOAA National Weather Service Radiosonde Observations. Retrieved 29/12/2013, 2013, from http://www.ua.nws.noaa.gov/factsheet.htm

Peters, T. M., Ott, D., & O'Shaughnessy, P. T. (2006). Comparison of the Grimm 1.108 and 1.109 portable aerosol spectrometer to the TSI 3321 aerodynamic particle sizer for dry particles. *Ann Occup Hyg, 50*(8), 843-850.

Pósfai, M., & Buseck, P. R. (2010). Nature and climate effects of individual tropospheric aerosol particles.

Ramana, M. V., Ramanathan, V., Kim, D., Roberts, G. C., & Corrigan, C. E. (2007). Albedo, atmospheric solar absorption and heating rate measurements with stacked UAVs. *Quarterly Journal of the Royal Meteorological Society, 133*(629), 1913-1931.

Raut, J. C., Chazette, P., & Fortain, A. (2009). Link between aerosol optical, microphysical and chemical measurements in an underground railway station in Paris. *Atmospheric Environment, 43*(4), 860-868.

Reggente, M., Mondini, A., Ferri, G., Mazzolai, B., Manzi, A., Gabelletti, M., . . . Lilienthal, A. J. (2010). The dustbot system: Using mobile robots to monitor pollution in pedestrian area. *Proc. of NOSE*.

Reiche, M., Roger Funk, Z. Z., Hoffmann, C., Li, Y., & Sommer, M. (2012). Using a Parafoil Kite for Measurement of Variations in Particulate Matter—A Kite-Based Dust Profiling Approach. *Atmospheric and Climate Sciences, 2*(1), 41-51.

Roberts, G. C., Ramana, M. V., Corrigan, C., Kim, D., & Ramanathan, V. (2008). Simultaneous observations of aerosol-cloud-albedo interactions with three stacked unmanned aerial vehicles. *Proc Natl Acad Sci U S A, 105*(21), 7370-7375.

Seaward, M. R. D. (1993). Lichens and sulphur dioxide air pollution: field studies. *Environmental Reviews, 1*(2), 73-91.

SHARP. (2006). SHARP GP2Y1010AU0F *Operation and Service Manual* (E4-A01501EN ed., pp. 9).

Silva, R. A., West, J. J., Zhang, Y., Anenberg, S. C., Lamarque, J. F., Shindell, D. T., . . . Folberth, G. (2013). Global premature mortality due to anthropogenic outdoor air pollution and the contribution of past climate change. *Environmental Research Letters, 8*(3), 034005.

Solomon, P. A., Moyers, J. L., & Fletcher, R. A. (1983). High-volume dichotomous virtual impactor for the fractionation and collection of particles according to aerodynamic size. *Aerosol science and Technology, 2*(4), 455-464.

Timoney, K. P., & Lee, P. (2009). Does the Alberta tar sands industry pollute? The scientific evidence. *Open Conservation Biology Journal, 3*, 65-81.

TSI. (2010). Model 8520 DUSTTRAK™ Aerosol Monitor *Operation and Service Manual* (1980198, Revision S ed., pp. 89). 500 Cardigan Road, Shoreview, MN 55126 U.S.A.

Twomey, S. (1977). The influence of pollution on the shortwave albedo of clouds. *Journal of the atmospheric sciences, 34*(7), 1149-1152.

van den Kroonenberg, A., Spieß, T., Buschmann, M., Martin, T., Anderson, P. S., Beyrich, F., & Bange, J. (2007). Boundary layer measurements with the autonomous mini-UAV M 2 AV. *Proceedings of DACH2007, Hamburg, Germany*, 10-14.

Wagner, J., & Leith, D. (2001). Passive aerosol sampler. Part I: Principle of operation. *Aerosol Science & Technology, 34*(2), 186-192.

Walesby, K. T., & Harrison, R. G. (2010). Note: A thermally stable tension meter for atmospheric soundings using kites. *Review of Scientific Instruments, 81*(7), 076104-076104-076103.

Wandinger, U., Müller, D., Böckmann, C., Althausen, D., Matthias, V., Bösenberg, J., . . . Stohl, A. (2002). Optical and microphysical characterization of biomass-burning and industrial-pollution aerosols from-multiwavelength lidar and aircraft measurements. *Journal of Geophysical Research: Atmospheres (1984–2012), 107*(D21), LAC 7-1-LAC 7-20.

William, L. (2013). CITIZENS' OBSERVATORY - Where does our air quality come from? *Meteorological International*, 126-128.

Zhu, K., Zhang, J., & Lioy, P. J. (2007). Evaluation and comparison of continuous fine particulate matter monitors for measurement of ambient aerosols. *Journal of the Air & Waste Management Association, 57*(12), 1499-1506.

# CHAPTER 4: CONCLUSIONS AND FUTURE DIRECTIONS

## 4 Summary of Conclusions and Contributions:

This thesis designed, tested and established the PoC of a new helicopter-based sUAS platform for measuring wind speed and particulate matter in the atmospheric boundary layer (ABL). Measuring these atmospheric parameters is important as they have direct effects on a number of key processes that impact humans, including: climate, wind energy, air quality, drifting snow, fog, among others. The overall key findings from this thesis include:

### 4.0 Chapter 2 Key Findings

Currently, atmospheric boundary layer wind measurements with sUASs have mostly employed fixed-wing platforms. With this study I believe the results show that there is a benefit to using a traditional helicopter platform. The sUAS and its custom wind measurement payload were commensurate with a conventional system. As demonstrated, wake effects are mitigated if the anemometer is positioned at the front of the aircraft, outside the realm of influence. In winds reaching up to 17 m/s the sUAS maintained its position to within a few meters vertical. A key scientific milestone of the research presented in Chapter 2 is the degree to which the commensurability of this new system was demonstrated. Expandability of the custom measurement and control system is possible, allowing for additional atmospheric parameters to be measured.

### 4.1 Chapter 3 Key Findings

Chapter 3 explored two major questions split into two phases. Phase 1 compared two particulate matter sensors; a commodity sensor (Sharp GP2Y1010AU0F), to a commonly used PM sensor (DustTrak 8520). Results comparing the sensors showed that the Sharp PM sensor is not commensurate to the DustTrak. Issues with the Sharp sensor were identified, which include variations in the performance of one Sharp sensor to another, the need to time-average

measurements to filter noise, and a low saturation limit. Due to these issues, the goal of developing a lightweight PM payload based on the Sharp sensor was not achieved.

In phase 2, the helicopter-based sUAS was developed to carry the DustTrak sensor and was tested. Field tests with a collocated tower showed a near 1:1 relation between the DustTrak PM measurements onboard the sUAS during hover, versus those from a second DustTrak at the same height on an adjacent tower. This confirms that the aircraft has little to no effect on the PM measurements during hover. During the PoC demonstration the sUAS and DustTrak measured vertical variations of PM mass concentration, and with the addition of the anemometer from Chapter 2, the PM flux was also determined. Therefore, this research demonstrates that it is possible to collect spatial measurements of airborne PM levels with an sUAS and PM sensor.

## 4.2 Future Directions

The experiments conducted in this thesis were designed to test a new platform combined with new measurement and control systems for measuring wind speed and PM in the ABL. There are many directions in which this research could be advanced, however I feel the next steps lie with advancement in the different technologies that encompasses the platform. These areas include a new power source to allow longer flight times, integration with the DJI flight control program to allow for automated heading updating paired with wind direction.

## Appendix 1: Arduino Program

```
#include <SimpleTimer.h>
#include <SoftwareSerial.h>
#include <LiquidCrystal.h>
#include <TinyGPS.h>
#include <Wire.h>
#include <Time.h>

//Display//
const int BACK_LIGHT = 13;
LiquidCrystal lcd(12, 11, 5, 4, 3, 2);

//Wind//
SimpleTimer timer;
int arrayCount = 0;
int numberStore = 0;
int count = 0;
int countHz = 0;
float startTime = 0;
float stopTime = 0;
int pin = 0;

//GPS//
TinyGPS gps;
SoftwareSerial serial_gps(10, 9);
float flat, flon, falt;
unsigned long fix_age, time, date, age;

void setup()
{
  pinMode(BACK_LIGHT, OUTPUT);
  digitalWrite(BACK_LIGHT, HIGH);
  Serial.begin(9600);
  Serial3.begin(9600);
  serial_gps.begin(9600);
  timer.setInterval(1000, Repeat);
  digitalWrite(21, HIGH);
  attachInterrupt(2, AnemometerPulseLow, FALLING);
}

void loop()
{
  while (serial_gps.available())
  {
    int c = serial_gps.read();
    if (gps.encode(c))
      {
        gps.f_get_position(&flat, &flon, &age);
        falt = gps.f_altitude();
        gps.get_datetime(&date, &time, &fix_age);
      }
  }
   timer.run();
}

void Repeat() {
  Serial.print("Repeat:");
  double speedFinal = count  * 0.5588;
  OutPut(speedFinal);
```

```
  count = 0;
}

void AnemometerPulseLow()
{
      noInterrupts();
      count++;
      interrupts();
      Serial.println(count);
}

void OutPut(float U){
  lcd.begin(16, 2);
    lcd.print("Wind Speed:");
    Serial3.print(U);
    lcd.print(U);
    Serial3.print(",");
    Serial3.print(time);
    Serial3.print(",");
    Serial3.print(flat == TinyGPS::GPS_INVALID_F_ANGLE ? 0.0 : flat, 6);
    Serial3.print(",");
    Serial3.print(flon == TinyGPS::GPS_INVALID_F_ANGLE ? 0.0 : flon, 6);
    Serial3.print(",");
    Serial3.print(falt);
    Serial3.print(",");
    Serial3.print("SAT=");
    Serial3.print(gps.satellites()    ==    TinyGPS::GPS_INVALID_SATELLITES    ?    0    :
gps.satellites());
    Serial3.print(",");
    Serial3.println(millis() / 1000);

    lcd.setCursor(0, 1);
    lcd.print("T=");
    lcd.print(time);
}
```

## Appendix 2: Arduino (MCS) Overview